ESTRELLAS BINARIAS

ESTRELLAS BINARIAS

Pares físicos (estrellas dobles) en los que las estrellas se mueve en torno al centro de masa del sistema, de acuerdo con las leyes de Kepler

ESTRELLAS BINARIAS

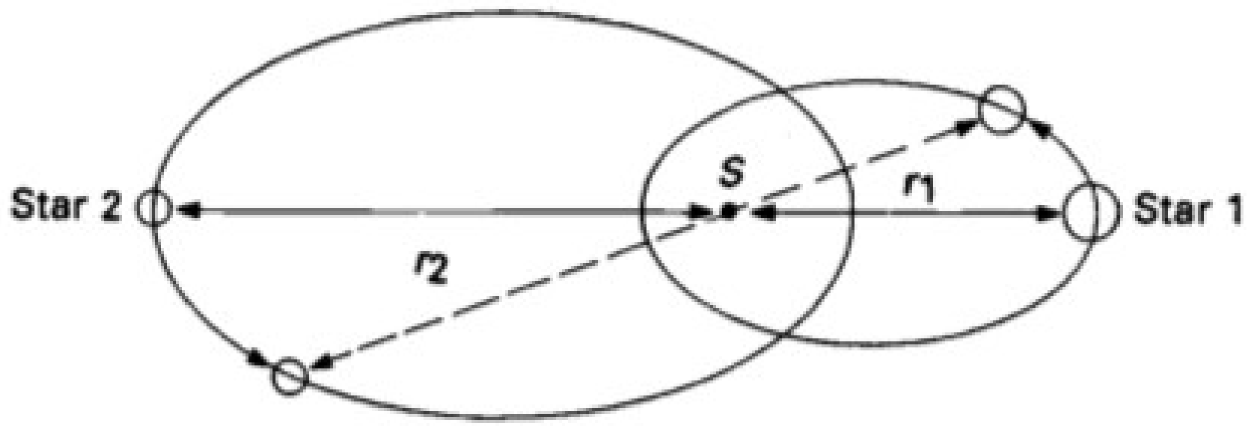

Fig. 9.1. In a binary system the two stars, Star 1 and Star 2 orbit their center of gravity, S.

Pares físicos (estrellas dobles) en los que las estrellas se mueven en torno al centro de masa del sistema, de acuerdo con las leyes de Kepler

→ derivar masas y radios en forma directa

→ 50 - 85 % estrellas binarias

ESTRELLAS BINARIAS

Pares físicos (estrellas dobles) en los que las estrellas se mueven en torno al centro de masa del sistema, de acuerdo con las leyes de Kepler → derivar masas y radios en forma directa.

→ 50 - 85 % estrellas binarias

Clasificación:

- Binarias visuales
- Binarias astrométricas
- Binarias fotométricas o eclipsantes
- Binarias espectroscópicas (uno/dos espectros visibles)

Falsas binarias
“estrellas dobles”

Mizar – Alcor (1650)

Binarias visuales

Se resuelven independientemente

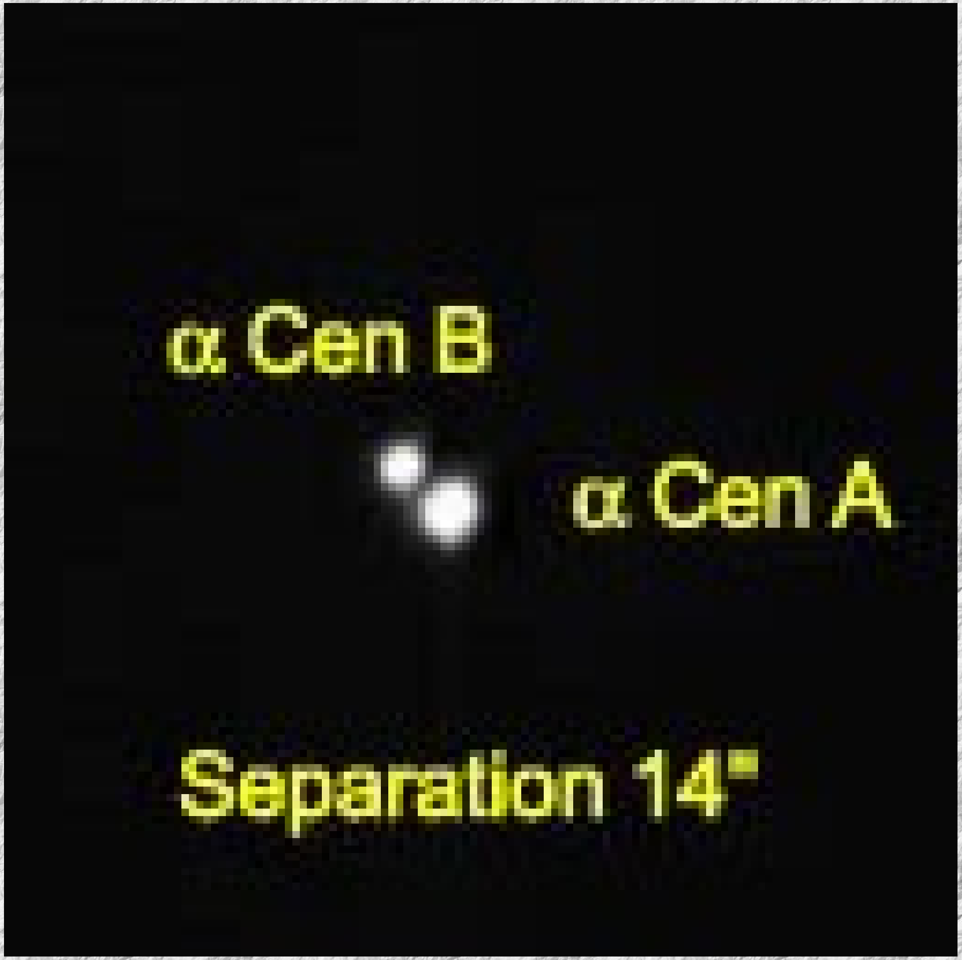

Binarias visuales

Se resuelven independientemente

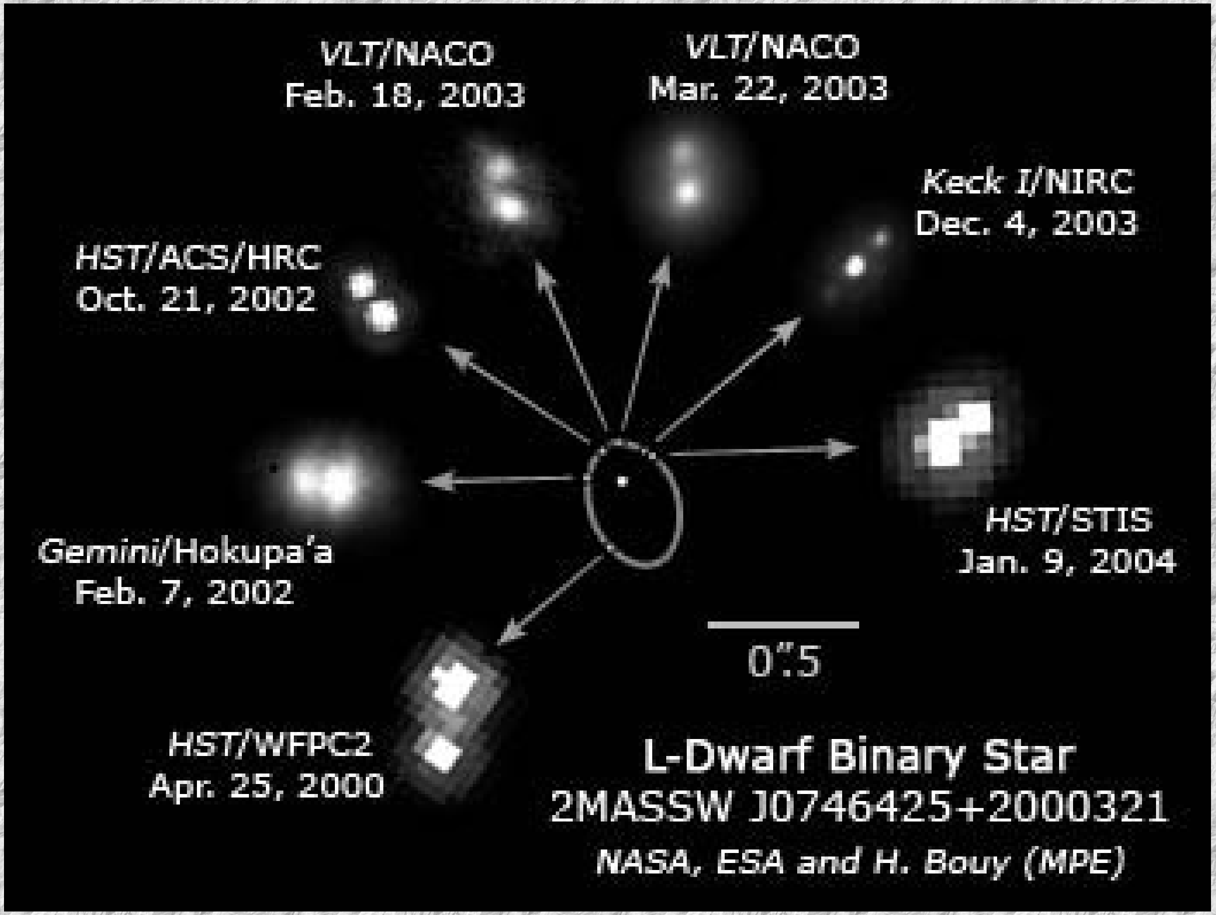

Binarias astrométricas

No es (era) posible observar ambas directamente

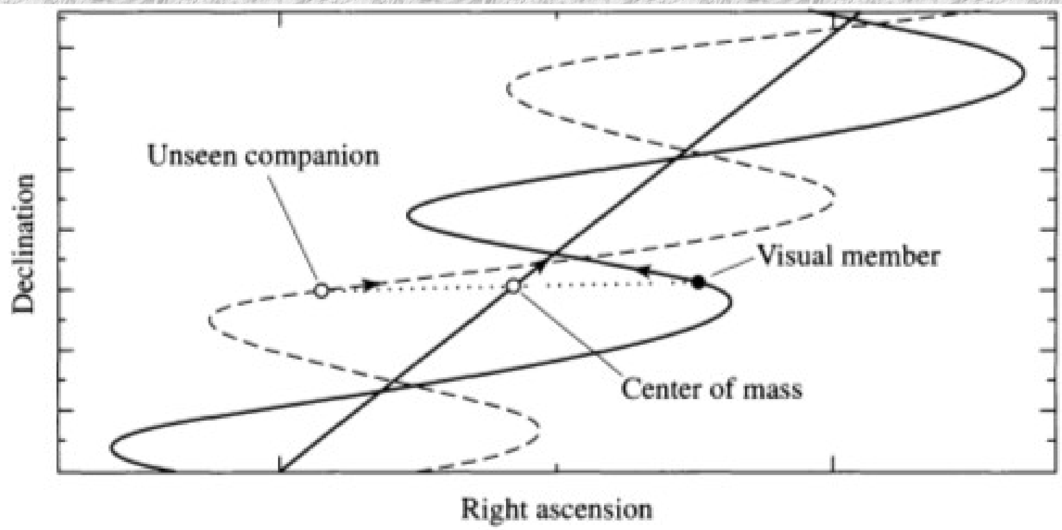

FIGURE 7.1 An astrometric binary, which contains one visible member. The unseen component is implied by the oscillatory motion of the observable star in the system. The proper motion of the entire system is reflected in the straight-line motion of the center of mass.

Binarias astrométricas

No es (era) posible observar ambas directamente

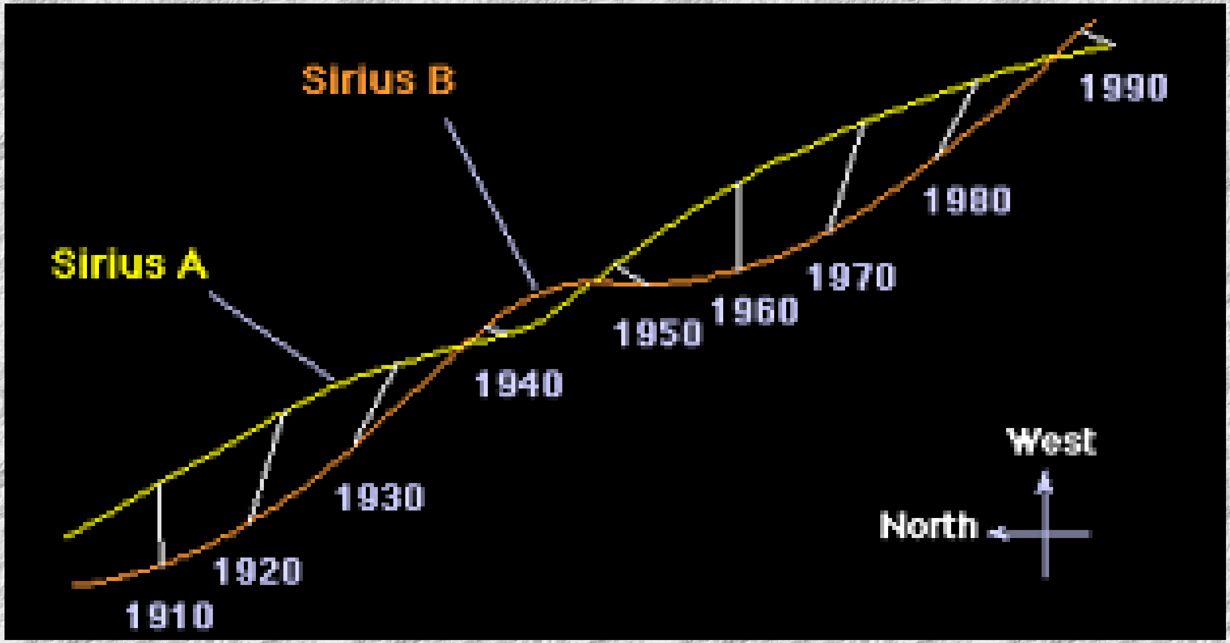

Binarias eclipsantes (fotométricas)

Variaciones **regulares** en la luz recibida

Binarias eclipsantes (fotométricas)

Variaciones regulares en la luz recibida

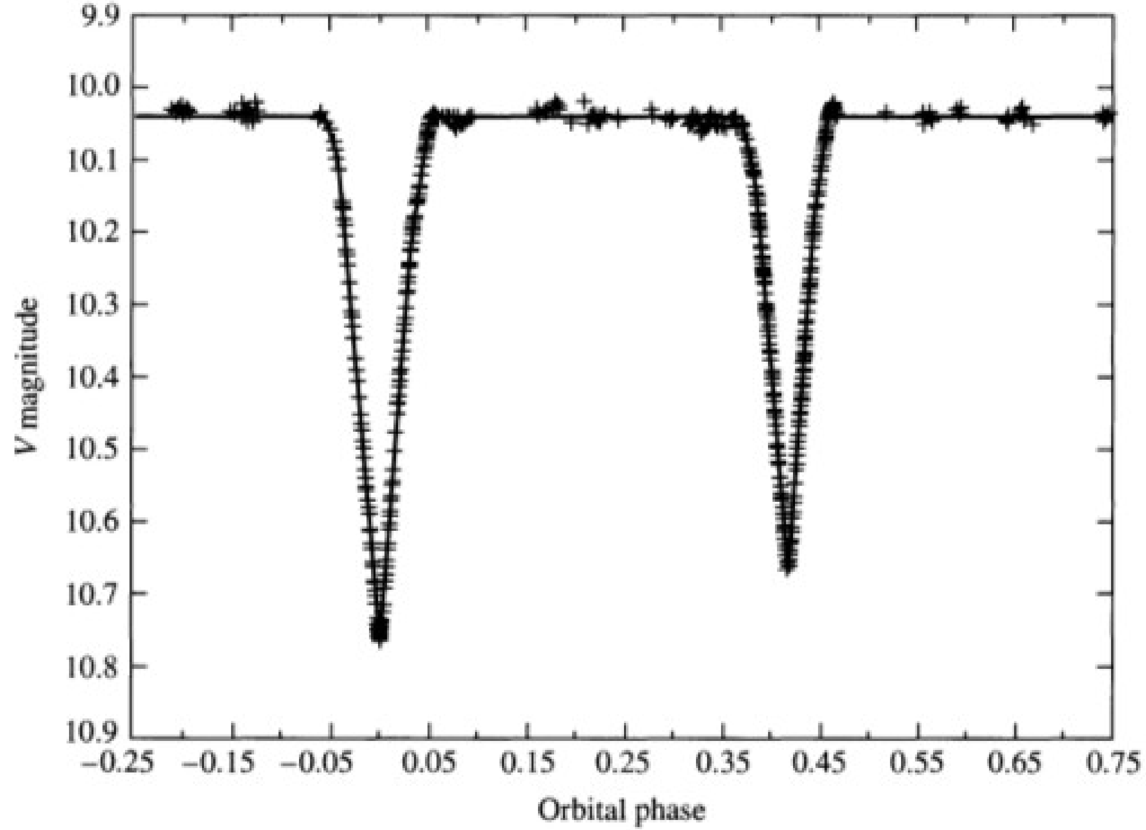

FIGURE 7.2 The V magnitude light curve of YY Sagittarii, an eclipsing binary star. The data from many orbital periods have been plotted on this light curve as a function of phase, where the phase is defined to be 0.0 at the primary minimum. This system has an orbital period $P = 2.6284734$ d, an eccentricity $e = 0.1573$, and orbital inclination $i = 88.89°$ (see Section 7.2). (Figure adopted from Lacy, C. H. S., *Astron. J.*, *105*, 637, 1993.)

Binarias eclipsantes (fotométricas)

Variaciones regulares en la luz recibida

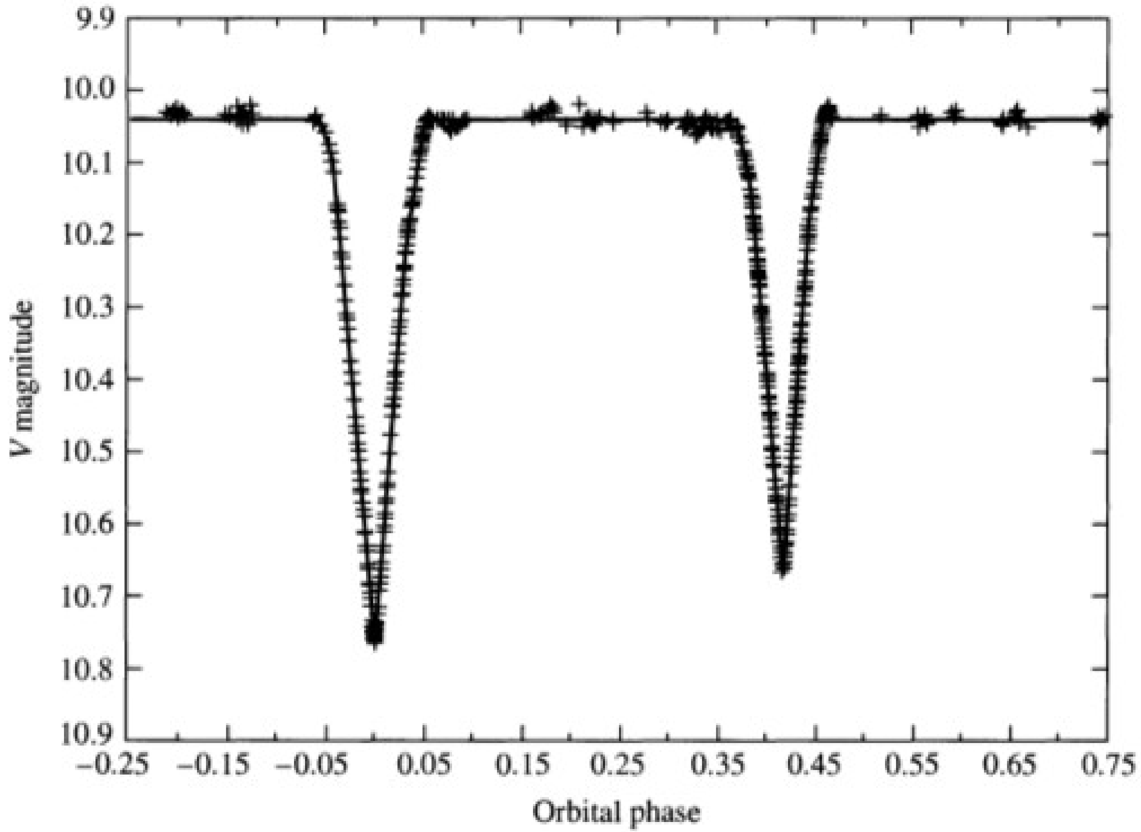

FIGURE 7.2 The V magnitude light curve of YY Sagittarii, an eclipsing binary star. The data from many orbital periods have been plotted on this light curve as a function of phase, where the phase is defined to be 0.0 at the primary minimum. This system has an orbital period $P = 2.6284734$ d, an eccentricity $e = 0.1573$, and orbital inclination $i = 88.89°$ (see Section 7.2). (Figure adopted from Lacy, C. H. S., *Astron. J.*, *105*, 637, 1993.)

Binarias espectroscópicas

Dos espectros superpuestos

(independientes y distinguibles)

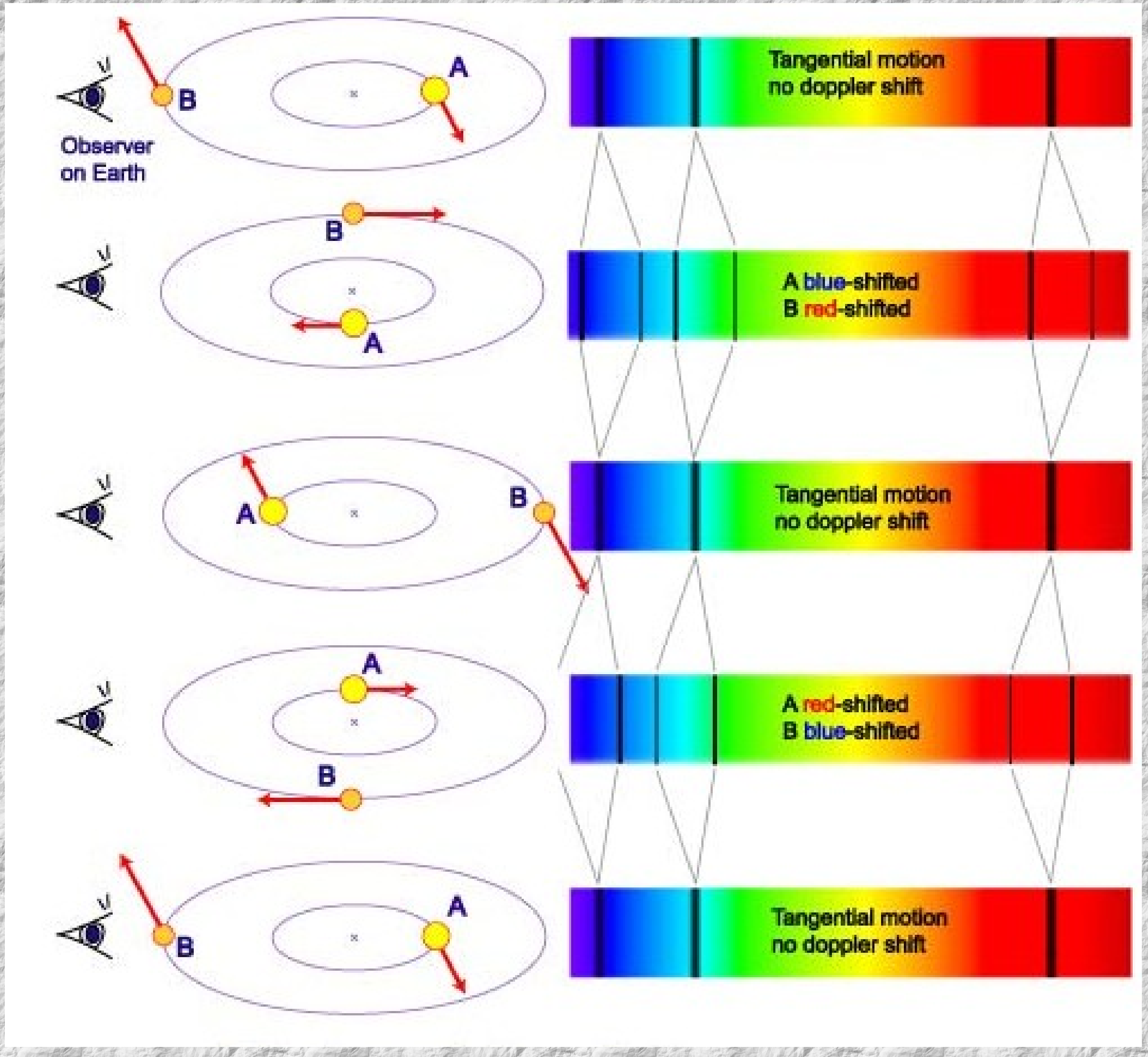

Binarias visuales

- Sirius A

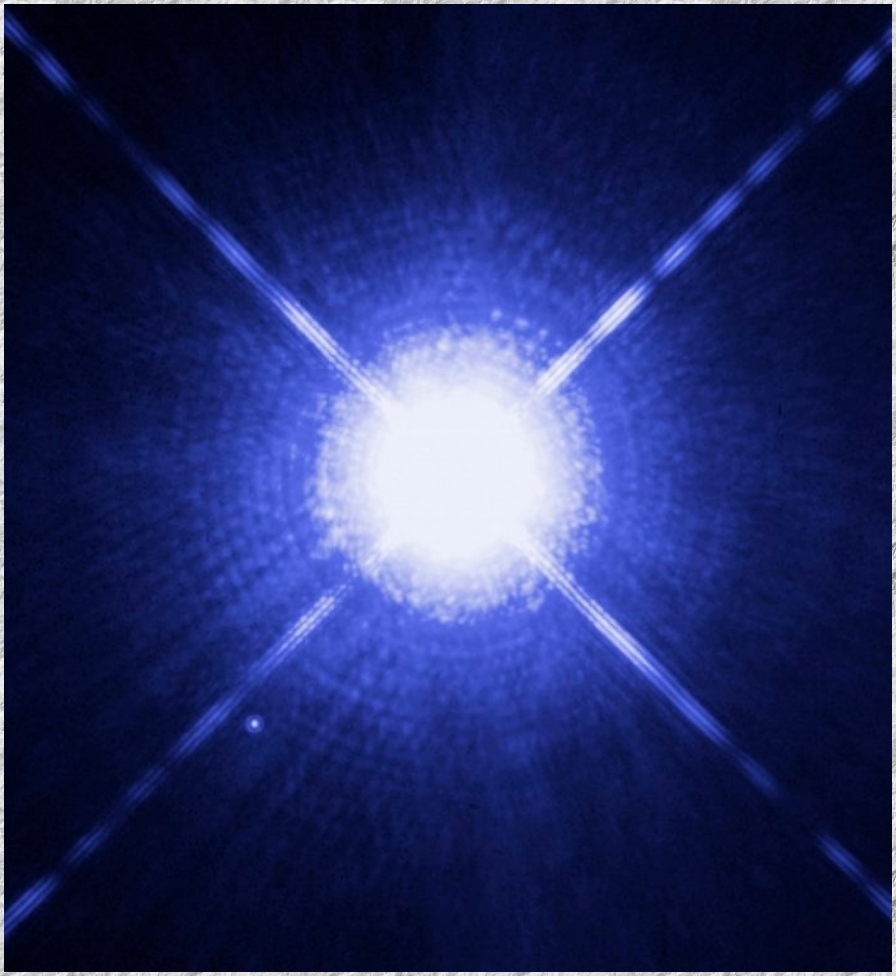

- Sirius B

Binarias visuales

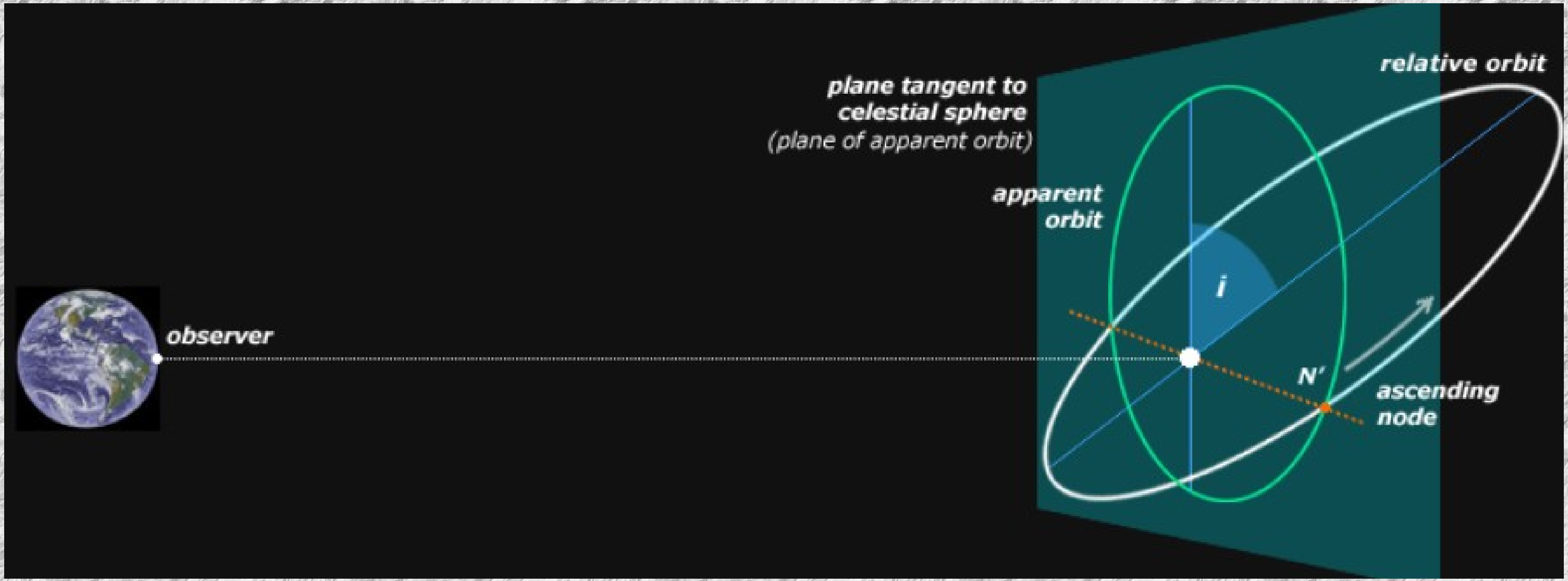

Binarias visuales
Determinación de masas

To see how a visual binary can yield mass information, consider two stars in orbit about their mutual center of mass. Assuming that the orbital plane is perpendicular to the observer's line of sight, we see from the discussion of Section 2.3 that the ratio of masses may be found from the ratio of the angular separations of the stars from the center of mass. Using Eq. (2.19) and considering only the lengths of the vectors $\mathbf{r}_1$ and $\mathbf{r}_2$, we find that

$$\frac{m_1}{m_2} = \frac{r_2}{r_1} = \frac{a_2}{a_1}, \tag{7.1}$$

where a_1 and a_2 are the semimajor axes of the ellipses. If the distance from the observer to

Binarias visuales

To see how a visual binary can yield mass information, consider two stars in orbit about their mutual center of mass. Assuming that the orbital plane is perpendicular to the observer's line of sight, we see from the discussion of Section 2.3 that the ratio of masses may be found from the ratio of the angular separations of the stars from the center of mass. Using Eq. (2.19) and considering only the lengths of the vectors $\mathbf{r}_1$ and $\mathbf{r}_2$, we find that

$$\frac{m_1}{m_2} = \frac{r_2}{r_1} = \frac{a_2}{a_1}, \tag{7.1}$$

where a_1 and a_2 are the semimajor axes of the ellipses. If the distance from the observer to

the binary star system is d, then the angles subtended by the semimajor axes are

$$\alpha_1 = \frac{a_1}{d} \qquad \text{and} \qquad \alpha_2 = \frac{a_2}{d},$$

where α_1 and α_2 are measured in radians. Substituting, we find that the mass ratio simply becomes

$$\boxed{\frac{m_1}{m_2} = \frac{\alpha_2}{\alpha_1}.} \tag{7.2}$$

Binarias visuales

$$P^2 = \frac{4\pi^2}{G\,(m_1 + m_2)} a^3,$$

gives the sum of the masses of the stars, provided that the semimajor axis (a) of the orbit of the reduced mass is known. Since $a = a_1 + a_2$ (the proof of this is left as an exercise), the semimajor axis can be determined directly only if the distance to the system has been determined. Assuming that d is known, $m_1 + m_2$ may be combined with m_1/m_2 to give each mass separately.

Binarias visuales

$$P^2 = \frac{4\pi^2}{G\,(m_1 + m_2)}a^3,$$

gives the sum of the masses of the stars, provided that the semimajor axis (a) of the orbit of the reduced mass is known. Since $a = a_1 + a_2$ (the proof of this is left as an exercise), the semimajor axis can be determined directly only if the distance to the system has been determined. Assuming that d is known, $m_1 + m_2$ may be combined with m_1/m_2 to give each mass separately.

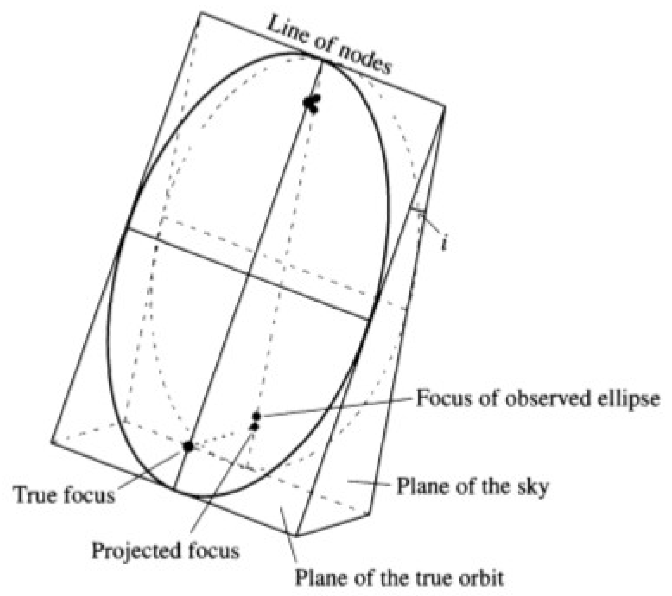

FIGURE 7.4 An elliptical orbit projected onto the plane of the sky produces an observable elliptical orbit. The foci of the original ellipse do not project onto the foci of the observed ellipse, however.

Binarias visuales

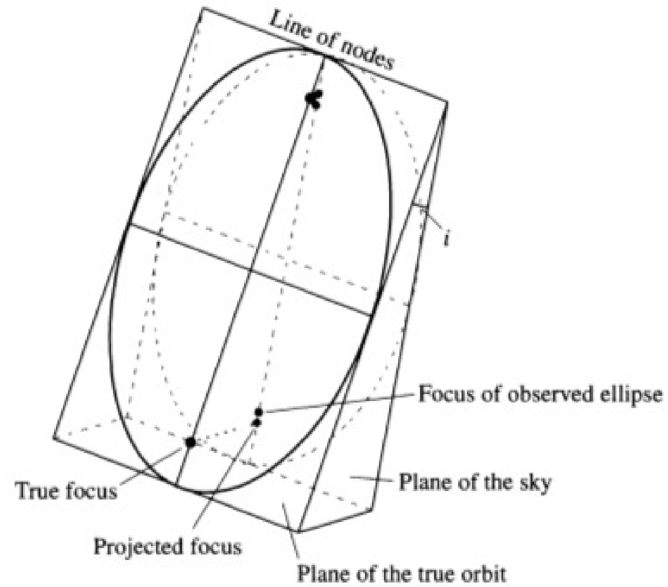

FIGURE 7.4 An elliptical orbit projected onto the plane of the sky produces an observable elliptical orbit. The foci of the original ellipse do not project onto the foci of the observed ellipse, however.

Let i be the **angle of inclination** between the plane of an orbit and the plane of the sky, as shown in Fig. 7.4; note that the orbits of both stars are necessarily in the same plane. As a special case, assume that the orbital plane and the plane of the sky (defined as being perpendicular to the line of sight) intersect along a line parallel to the minor axis, forming a **line of nodes**. The observer will not measure the actual angles subtended by the semimajor axes α_1 and α_2 but their projections onto the plane of the sky, $\tilde{\alpha}_1 = \alpha_1 \cos i$ and $\tilde{\alpha}_2 = \alpha_2 \cos i$. This geometrical effect plays no role in calculating the mass ratios since the $\cos i$ term will simply cancel in Eq. (7.2):

$$\frac{m_1}{m_2} = \frac{\alpha_2}{\alpha_1} = \frac{\alpha_2 \cos i}{\alpha_1 \cos i} = \frac{\tilde{\alpha}_2}{\tilde{\alpha}_1}.$$

However, this projection effect can make a significant difference when we are using Kepler's third law. Since $\alpha = a/d$ (α in radians), Kepler's third law may be solved for the sum of

Binarias visuales

Let i be the **angle of inclination** between the plane of an orbit and the plane of the sky, as shown in Fig. 7.4; note that the orbits of both stars are necessarily in the same plane. As a special case, assume that the orbital plane and the plane of the sky (defined as being perpendicular to the line of sight) intersect along a line parallel to the minor axis, forming a **line of nodes**. The observer will not measure the actual angles subtended by the semimajor axes α_1 and α_2 but their projections onto the plane of the sky, $\tilde{\alpha}_1 = \alpha_1 \cos i$ and $\tilde{\alpha}_2 = \alpha_2 \cos i$. This geometrical effect plays no role in calculating the mass ratios since the $\cos i$ term will simply cancel in Eq. (7.2):

$$\frac{m_1}{m_2} = \frac{\alpha_2}{\alpha_1} = \frac{\alpha_2 \cos i}{\alpha_1 \cos i} = \frac{\tilde{\alpha}_2}{\tilde{\alpha}_1}.$$

However, this projection effect can make a significant difference when we are using Kepler's third law. Since $\alpha = a/d$ (α in radians), Kepler's third law may be solved for the sum of

$$\boxed{m_1 + m_2 = \frac{4\pi^2}{G}\frac{(\alpha d)^3}{P^2} = \frac{4\pi^2}{G}\left(\frac{d}{\cos i}\right)^3 \frac{\tilde{\alpha}^3}{P^2},} \tag{7.3}$$

Binarias eclipsantes

Variación periódica del brillo: no es intrínseca

→ las dos componentes se eclipsan mutuamente en su movimiento orbital en torno al CM.

Binarias eclipsantes

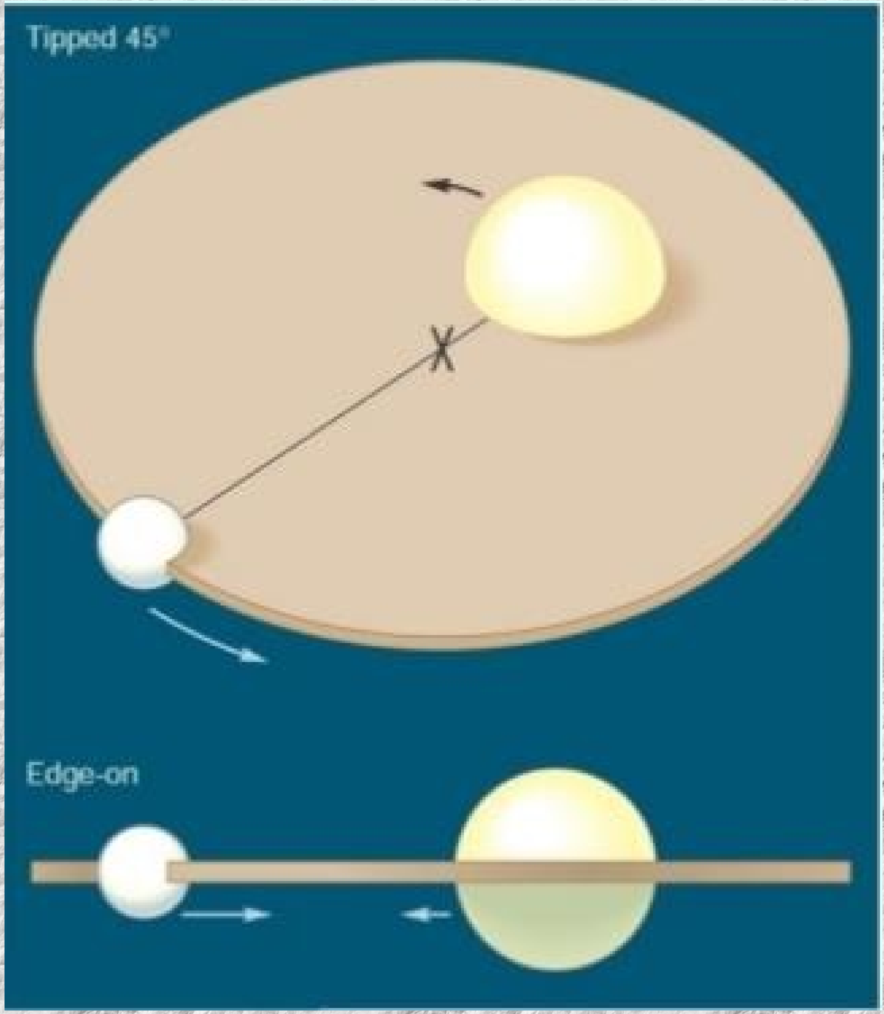

Binarias eclipsantes

- Variación periódica del brillo: no es intrínseca → las dos componentes se eclipsan mutuamente en su movimiento orbital en torno al CM.

- Variaciones → fotometría → magnitud (tiempo).

- La representación gráfica de las observaciones: **curva de luz.**

- Curva de luz: se caracteriza por la presencia de dos mínimos en cada período.

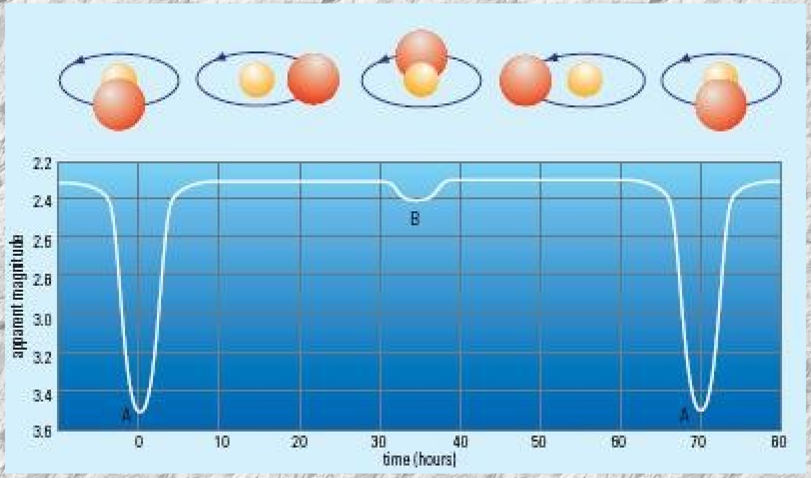

Periodo

Binarias eclipsantes

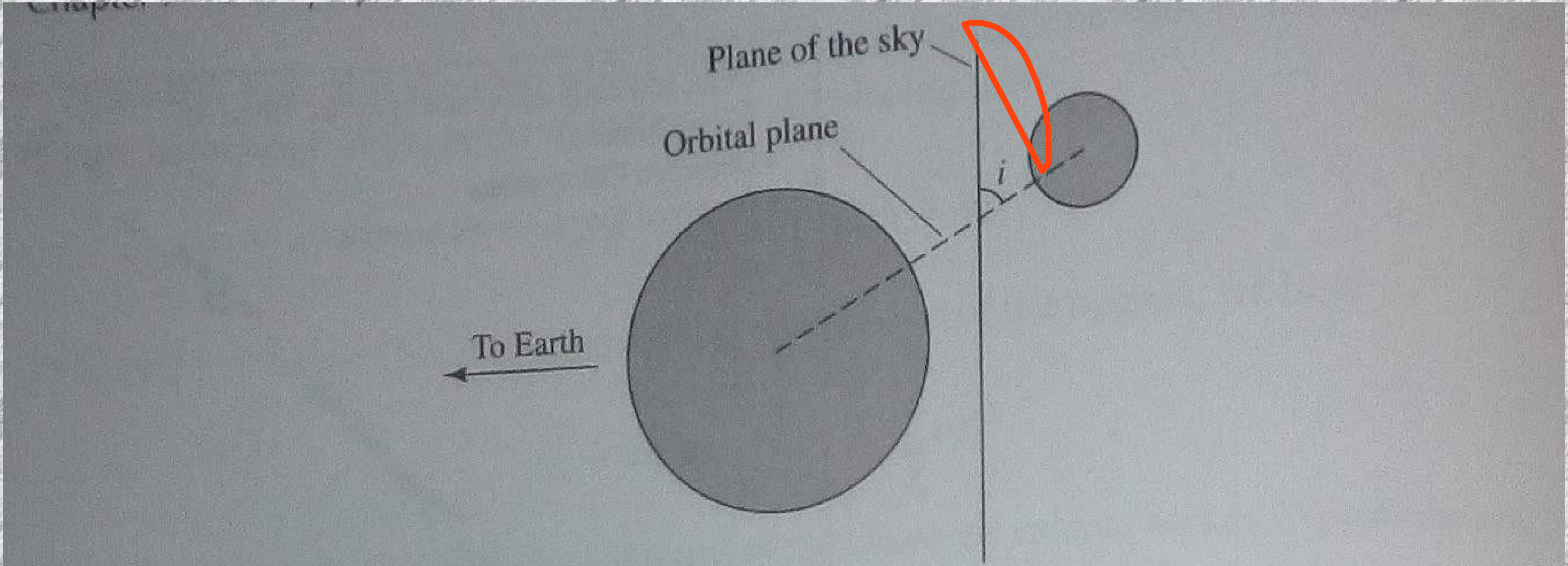

FIGURE 7.8 The geometry of an eclipsing, spectroscopic binary requires that the angle of inclination i be close to 90°.

tion i be close to 90°.

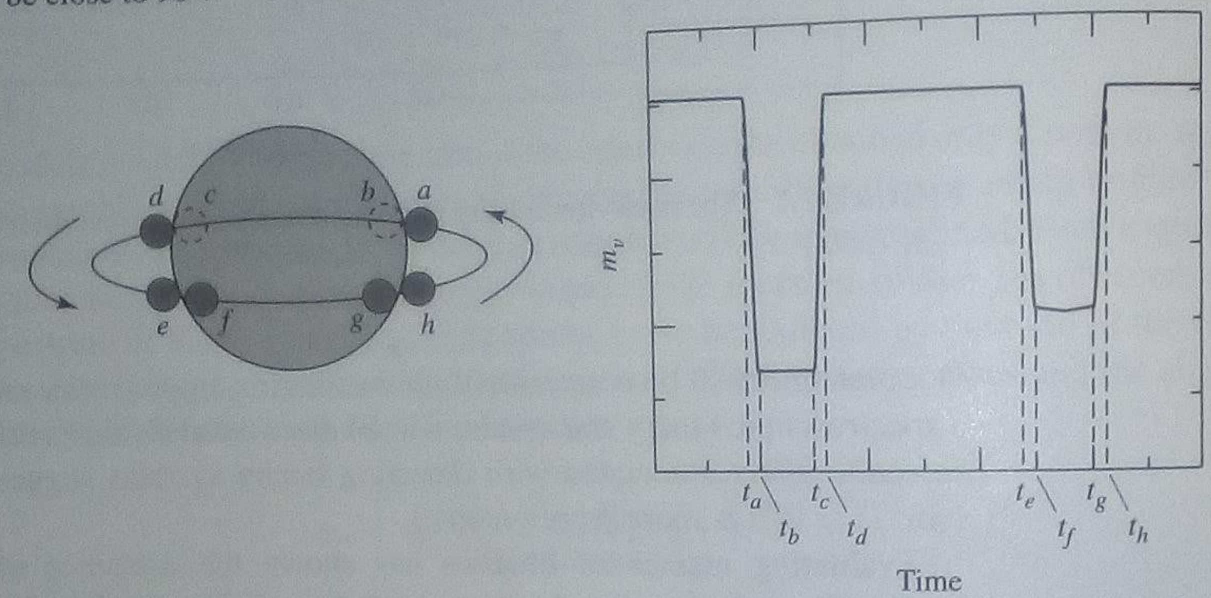

FIGURE 7.9 The light curve of an eclipsing binary for which $i = 90°$. The times indicated on the light curve correspond to the positions of the smaller star relative to its larger companion. It is assumed in this example that the smaller star is hotter than the larger one.

tion i be close to 90°.

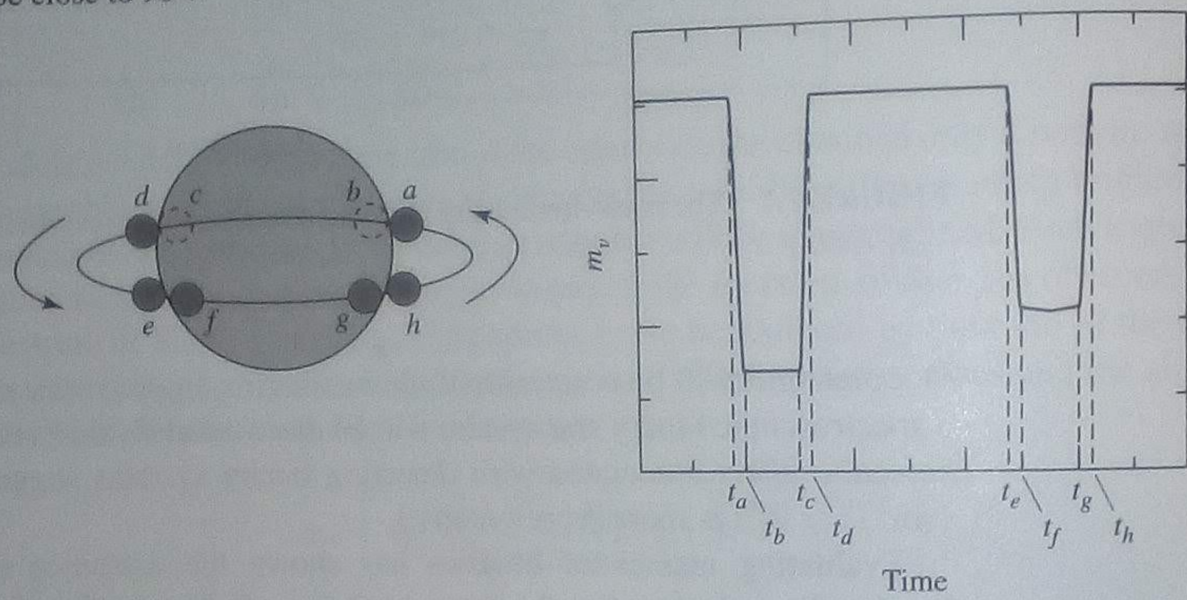

FIGURE 7.9 The light curve of an eclipsing binary for which $i = 90°$. The times indicated on the light curve correspond to the positions of the smaller star relative to its larger companion. It is assumed in this example that the smaller star is hotter than the larger one.

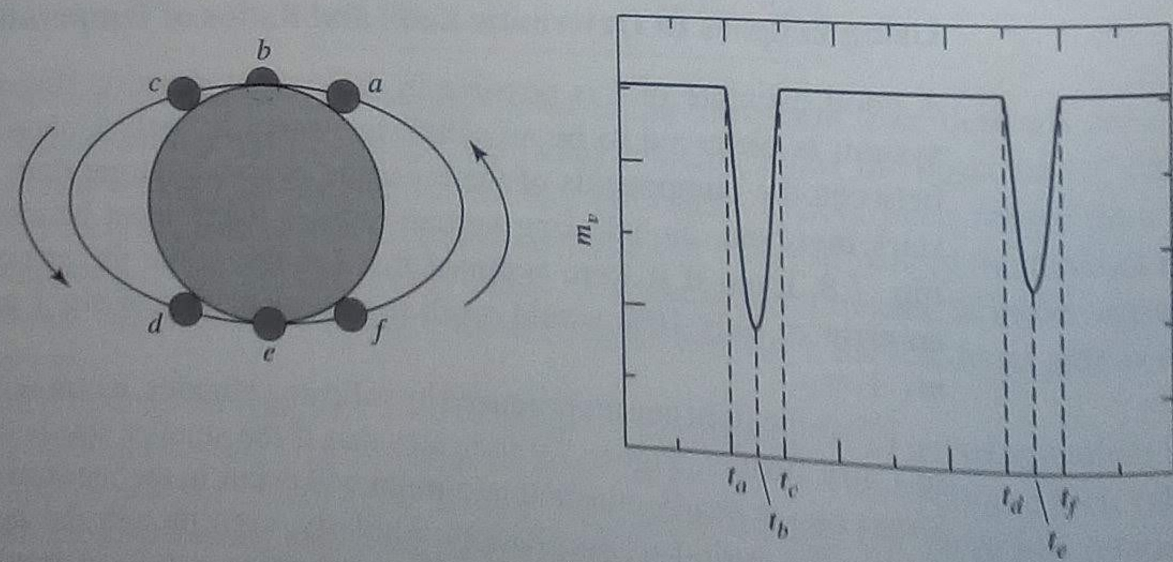

FIGURE 7.10 The light curve of a partially eclipsing binary. It is assumed in this example that the smaller star is hotter than its companion.

Binarias eclipsantes

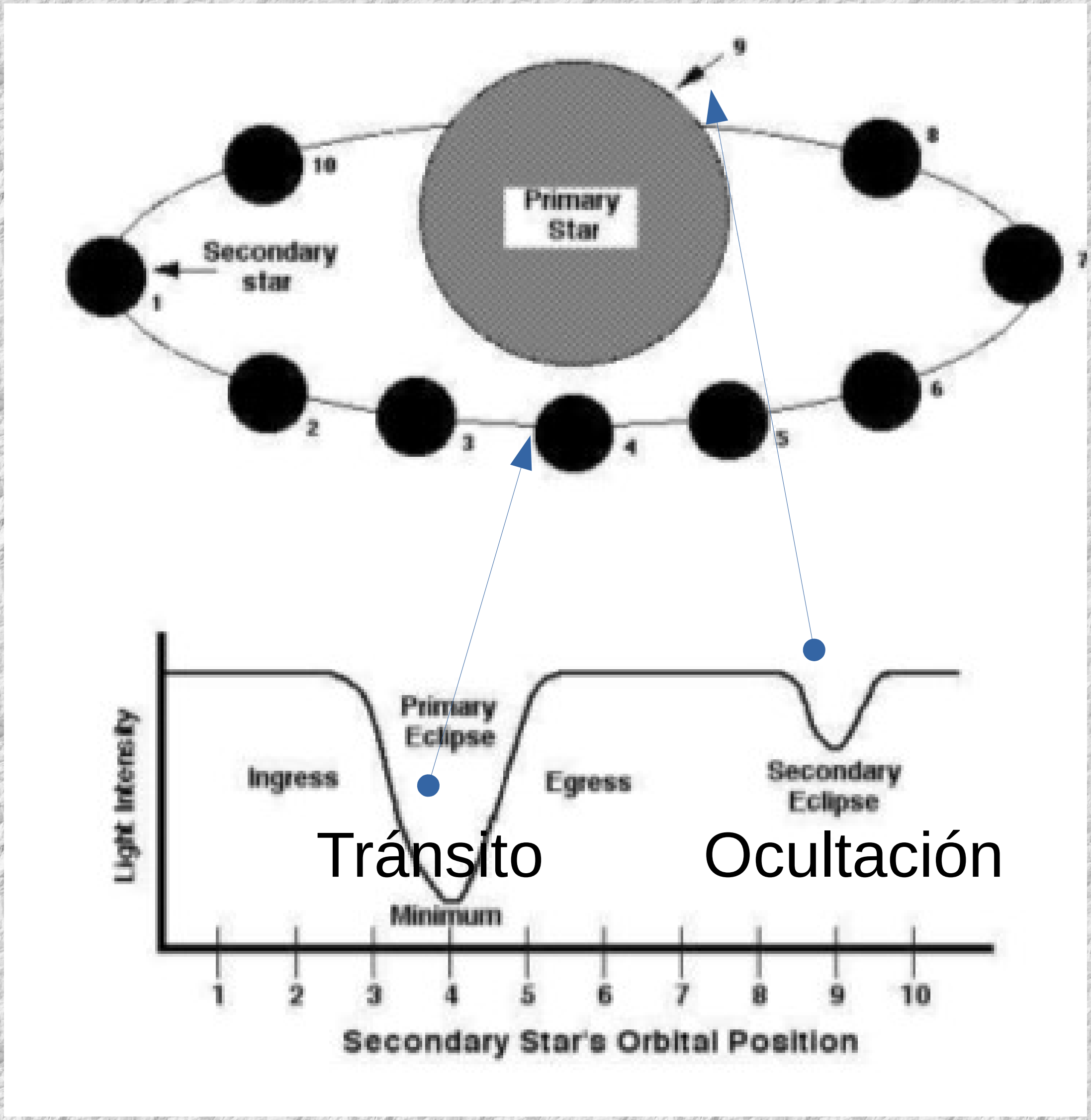

Estrella de mayor tamaño: mayor temperatura

Binarias eclipsantes

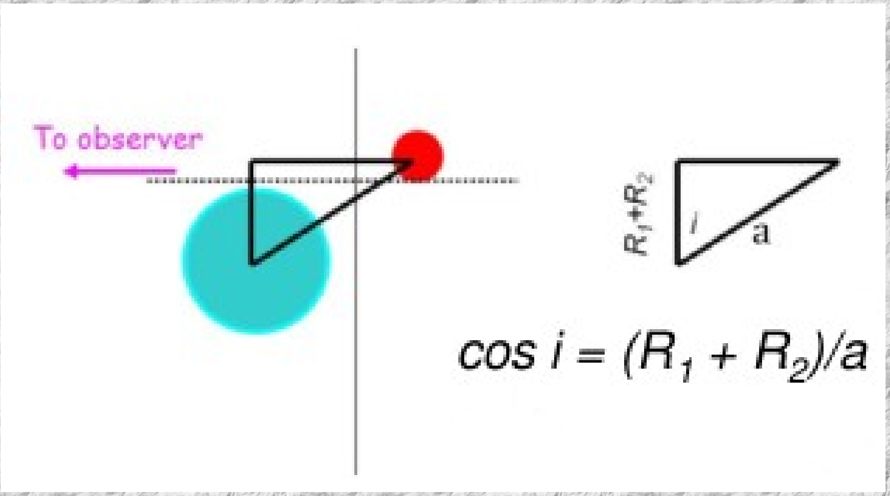

Binarias eclipsantes

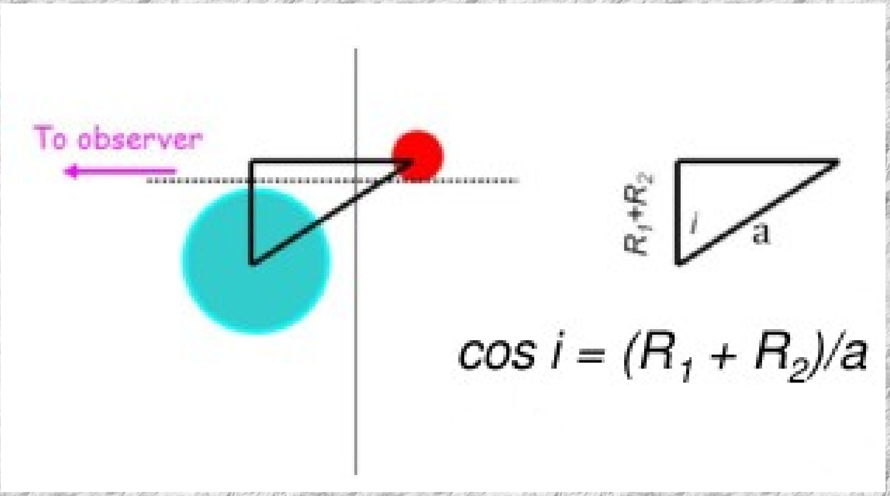

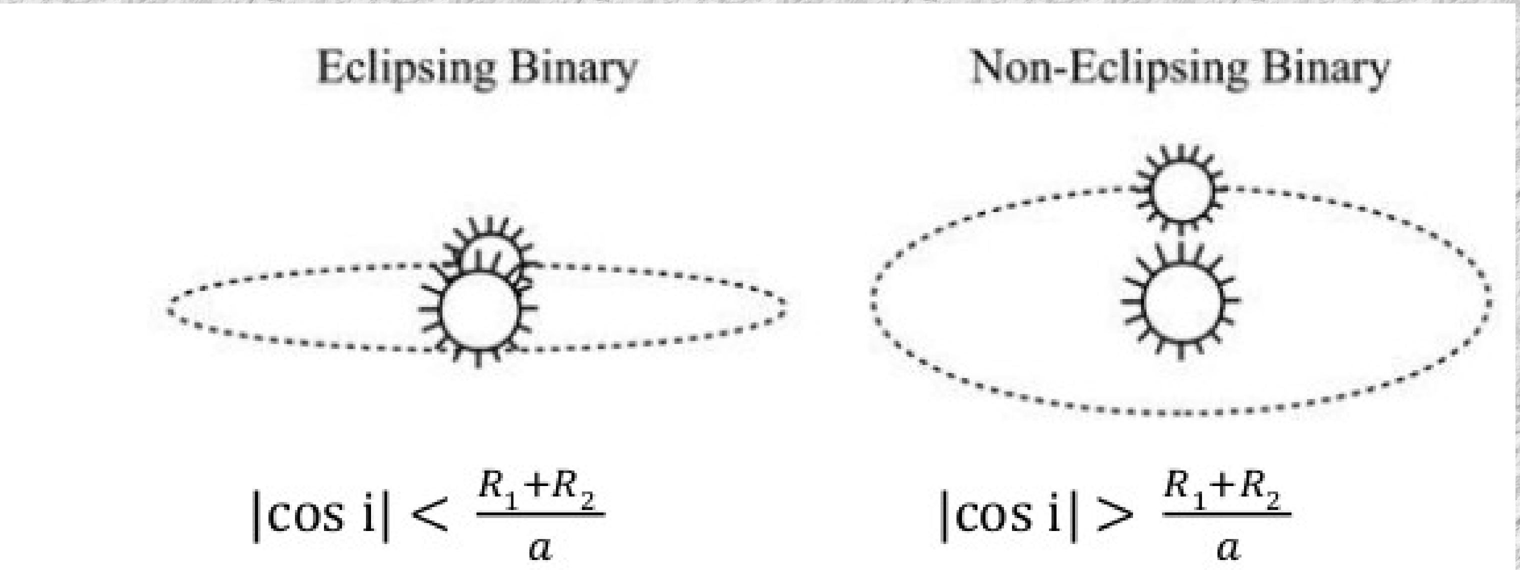

Binarias eclipsantes

where R_A and R_B are the radii of stars A and B respectively, and r is the orbital radius of star A around star B. Equation (9.15) assumes that star B is much more massive than star A such that the velocity of star B can be neglected. It also assumes $r \gg R_A$ and R_B.

(a)

Binarias eclipsantes

Radios relativos

$$t_e/P = \frac{2R_A + 2R_B}{2\pi r},$$

where R_A and R_B are the radii of stars A and B respectively, and r is the orbital radius of star A around star B. Equation (9.15) assumes that star B is much more massive than star A such that the velocity of star B can be neglected. It also assumes $r \gg R_A$ and R_B.

$$V_{r(\max)} = 2\pi r_A/P. \qquad (9.16)$$

$$t_t/P = (2R_B - 2R_A)/2\pi r_A. \qquad (9.17)$$

if again the mass of star B is much larger than the mass of star A. Equation (9.16) determines the orbital radius r_A. From (9.15) and (9.17) we obtain

$$(t_e - t_t)/P = \frac{4R_A}{2\pi r_A} \qquad (9.18)$$

and

$$(t_e + t_t)/P = \frac{4R_B}{2\pi r_A}. \qquad (9.19)$$

These equations determine the radii of both stars.

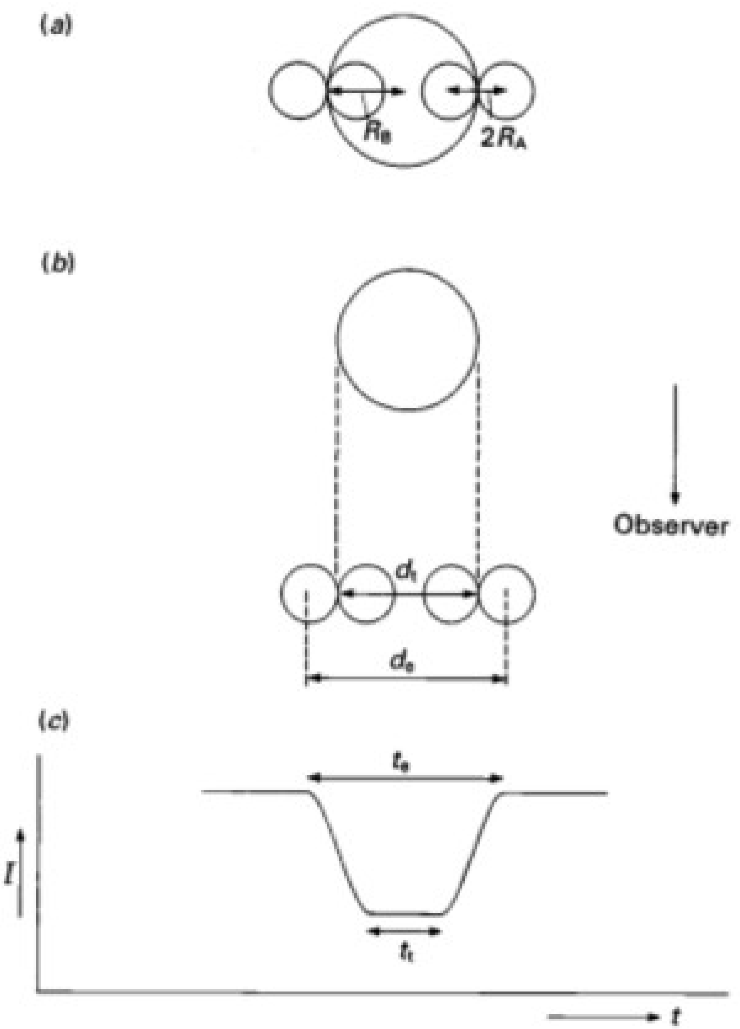

Fig. 9.14. Figure (a) shows the positions of the eclipsing star at first, second, third, and fourth contact as seen from an observer above the plane of the paper. Figure (b) shows the geometry of the eclipse for an observer whose line of sight is in the orbital plane (which is the plane of the paper), not drawn to scale. For a large distance between stars A and B the path of star B can be approximated by a straight line. Figure (c) shows the light curve as a function of time for the duration of the eclipse. During the time t_e star A travels a distance $d_e = 2R_A + 2R_B$. During the time t_t star A travels the distance $d_t = 2R_B - 2R_A$.

Binarias eclipsantes

Radios relativos

$$t_e/P = \frac{2R_A + 2R_B}{2\pi r},$$

where R_A and R_B are the radii of stars A and B respectively, and r is the orbital radius of star A around star B. Equation (9.15) assumes that star B is much more massive than star A such that the velocity of star B can be neglected. It also assumes $r \gg R_A$ and R_B.

$$V_{r(\max)} = 2\pi r_A/P. \qquad (9.16)$$

$$t_t/P = (2R_B - 2R_A)/2\pi r_A. \qquad (9.17)$$

if again the mass of star B is much larger than the mass of star A. Equation (9.16) determines the orbital radius r_A. From (9.15) and (9.17) we obtain

$$(t_e - t_t)/P = \frac{4R_A}{2\pi r_A} \qquad (9.18)$$

and

$$(t_e + t_t)/P = \frac{4R_B}{2\pi r_A}. \qquad (9.19)$$

These equations determine the radii of both stars.

If stars A and B have comparable masses we have to consider the motions of both stars. The eclipse times will then be shorter, because the relative velocities of the two stars will be larger, namely $V_A + V_B$, with $V_A = 2\pi r_A/P$ and $V_B = 2\pi r_B/P$.

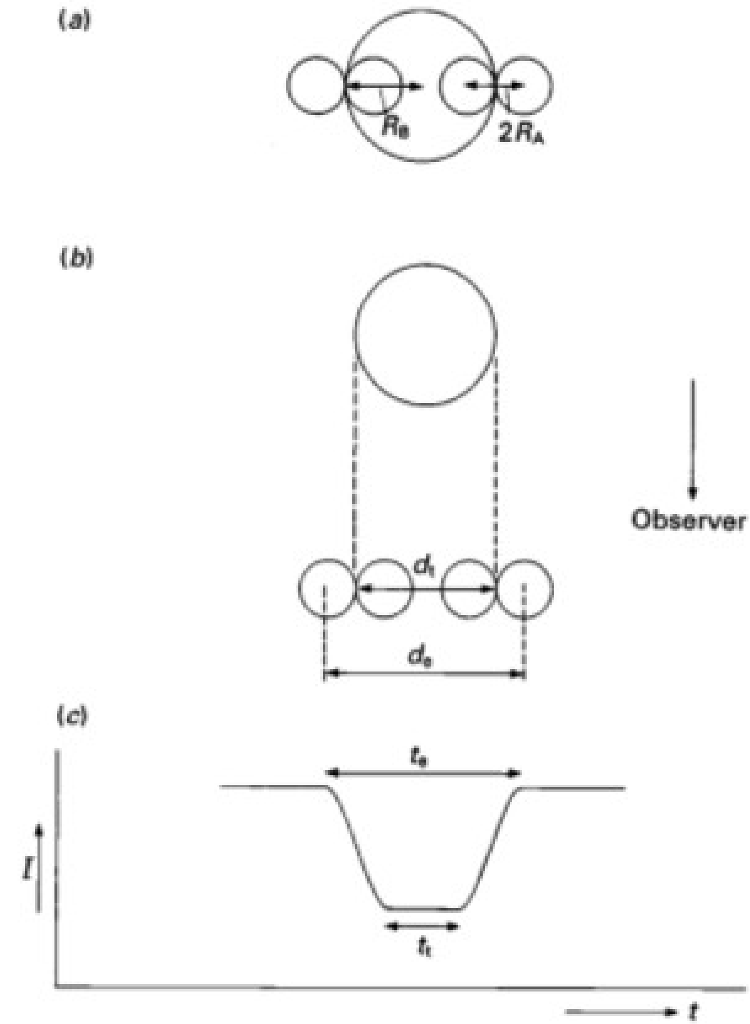

Fig. 9.14. Figure (*a*) shows the positions of the eclipsing star at first, second, third, and fourth contact as seen from an observer above the plane of the paper. Figure (*b*) shows the geometry of the eclipse for an observer whose line of sight is in the orbital plane (which is the plane of the paper), not drawn to scale. For a large distance between stars A and B the path of star B can be approximated by a straight line. Figure (*c*) shows the light curve as a function of time for the duration of the eclipse. During the time t_e star A travels a distance $d_e = 2R_A + 2R_B$. During the time t_t star A travels the distance $d_t = 2R_B - 2R_A$.

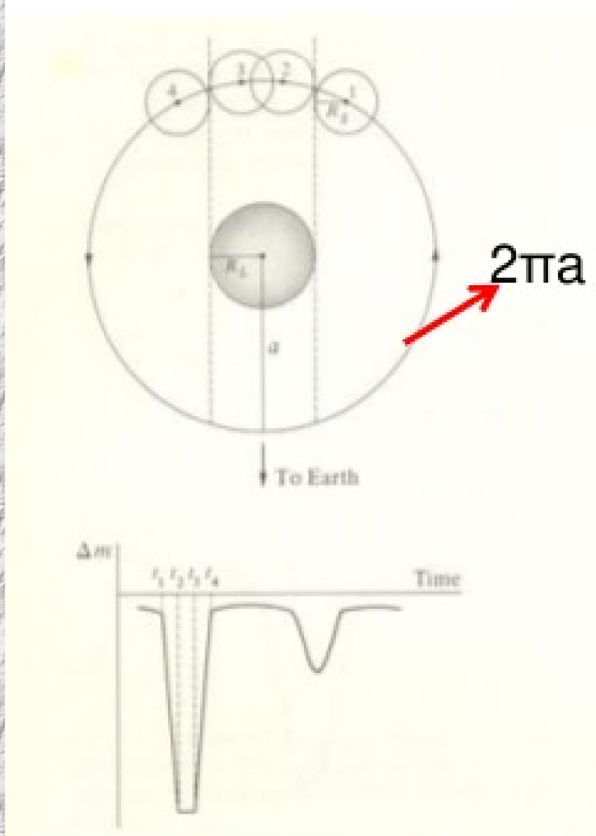

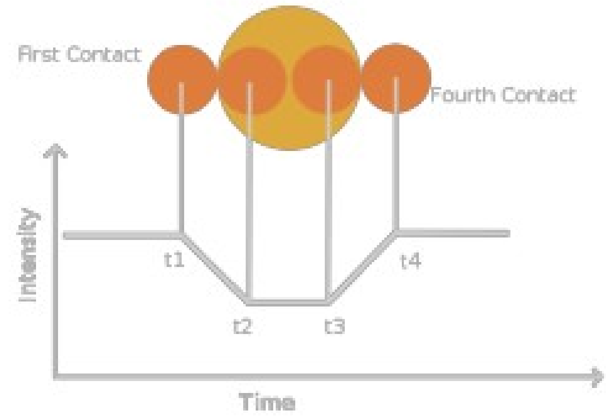

$$\frac{t_4 - t_1}{\mathscr{P}} \approx \frac{2(R_L + R_S)}{2\pi a}$$

$$\frac{t_3 - t_2}{\mathscr{P}} \approx \frac{2(R_L - R_S)}{2\pi a}.$$

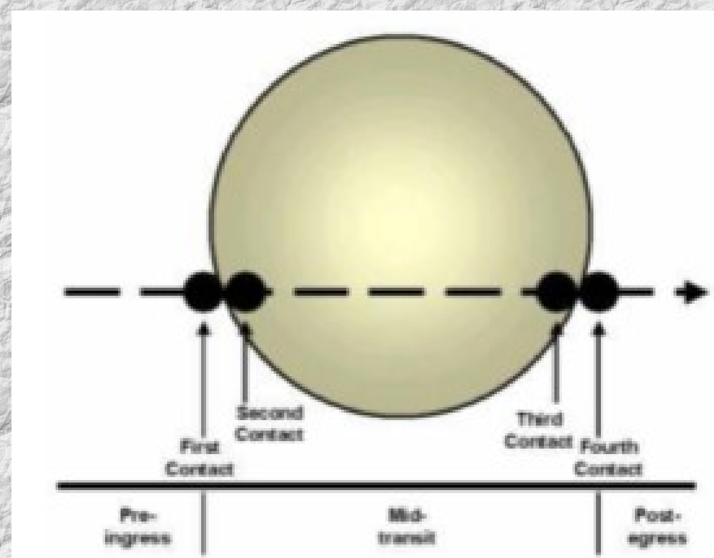

Binarias eclipsantes (fotométricas)

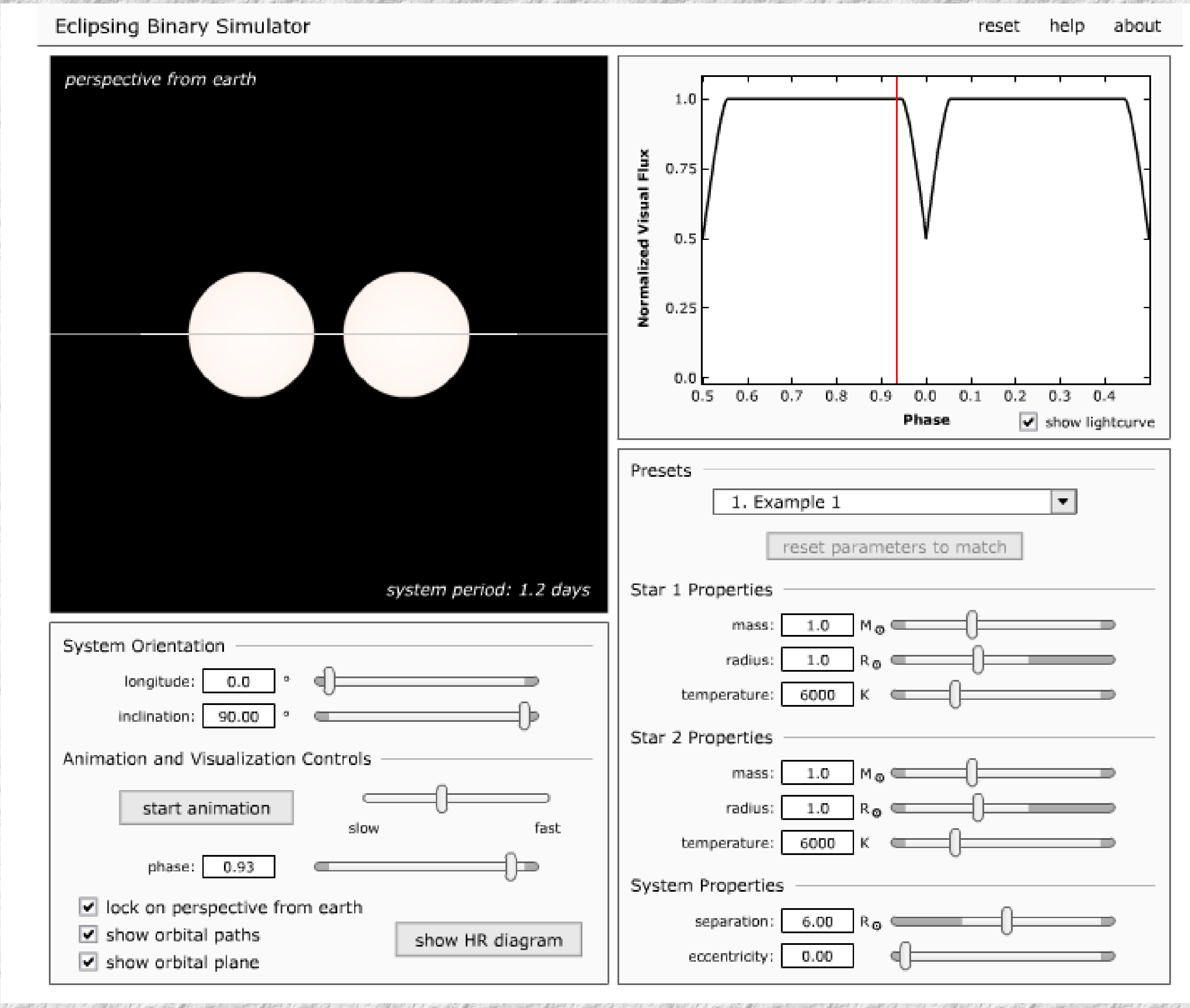

https://ccnmtl.github.io/astro-simulations/eclipsing-binary-simulator/

Brillo superficial de las binarias eclipsantes

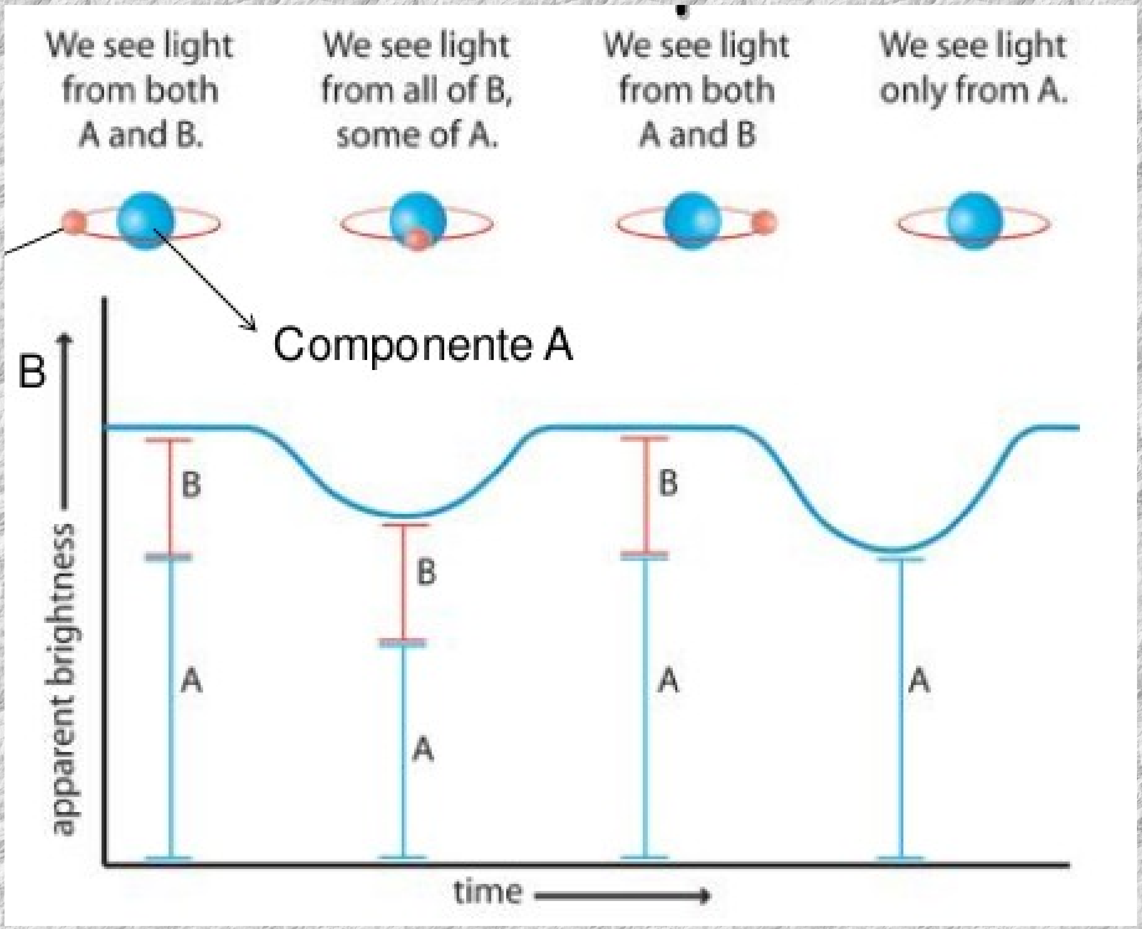

"La razón de los flujos medidos en los eclipses primario y secundario es proporcional el cociente de sus temperaturas"

Binarias eclipsantes

$$I_{max} = (\pi R_B^2 \cdot F_B + \pi R_A^2 \cdot F_A)\text{const.}$$

ne first eclipse the minimum intensity I_1 is given by

$$I_1 = [(\pi R_B^2 - \pi R_A^2) \cdot F_B + \pi R_A^2 \cdot F_A]\text{const.}.$$

the second eclipse the minimum intensity I_2 is giv

$$I_2 = (\pi R_B^2 \cdot F_B)\text{const.}.$$

his we derive

$$I_{max} - I_2 = (\pi R_A^2 \cdot F_A)\text{const.}$$

$$I_{max} - I_1 = (\pi R_A^2 \cdot F_B)\text{const.}.$$

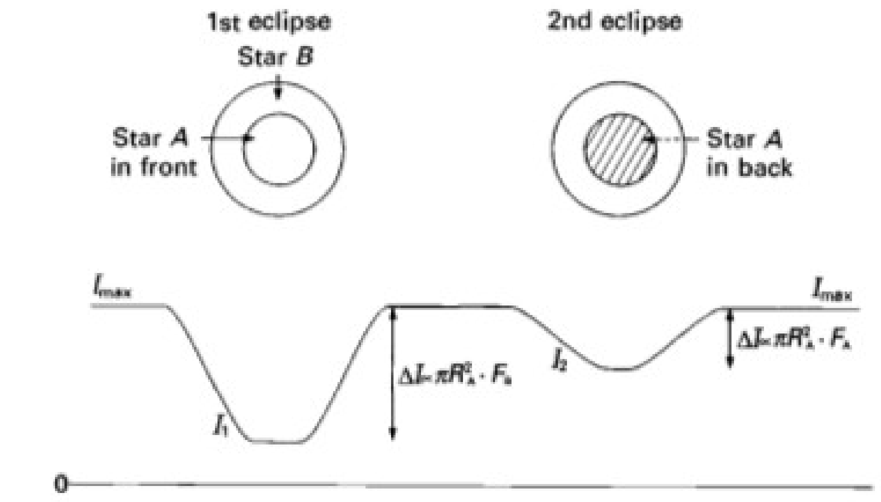

Fig. 9.15. During the first eclipse a fraction of the surface of star B is occulted. During the second eclipse star A is completely covered up. The depths of the light minima depend on the surface fluxes of star A and star B.

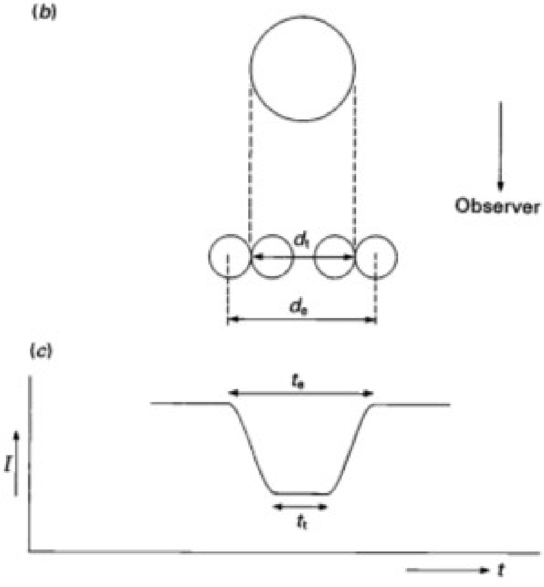

Fig. 9.14. Figure (a) shows the positions of the eclipsing star at first, second, third, and fourth contact as seen from an observer above the plane of the paper. Figure (b) shows the geometry of the eclipse for an observer whose line of sight is in the orbital plane (which is the plane of the paper), not drawn to scale. For a large distance between stars A and B the path of star B can be approximated by a straight line. Figure (c) shows the light curve as a function of time for the duration of the eclipse. During the time t_e star A travels a distance $d_e = 2R_A + 2R_B$. During the time t_t star A travels the distance $d_t = 2R_B - 2R_A$.

Binarias eclipsantes

$$I_{max} = (\pi R_B^2 \cdot F_B + \pi R_A^2 \cdot F_A)\text{const.}$$

he first eclipse the minimum intensity I_1 is given by

$$I_1 = [(\pi R_B^2 - \pi R_A^2) \cdot F_B + \pi R_A^2 \cdot F_A]\text{const.}.$$

the second eclipse the minimum intensity I_2 is giv

$$I_2 = (\pi R_B^2 \cdot F_B)\text{const.}.$$

his we derive

$$I_{max} - I_2 = (\pi R_A^2 \cdot F_A)\text{const.}$$

$$I_{max} - I_1 = (\pi R_A^2 \cdot F_B)\text{const.}.$$

$$\frac{I_{max} - I_2}{I_{max} - I_1} = \frac{F_A}{F_B}. \qquad (9.25)$$

If we know the flux for one star, we can determine the flux of the other star. Since the radiative fluxes F_A and F_B determine the effective temperatures of the stars we can also determine the ratio of the effective temperatures of the two components of an eclipsing binary system.

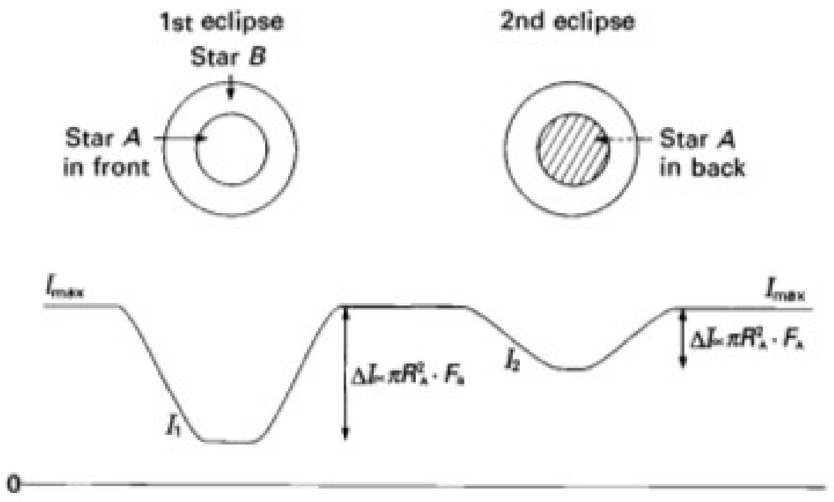

Fig. 9.15. During the first eclipse a fraction of the surface of star B is occulted. During the second eclipse star A is completely covered up. The depths of the light minima depend on the surface fluxes of star A and star B.

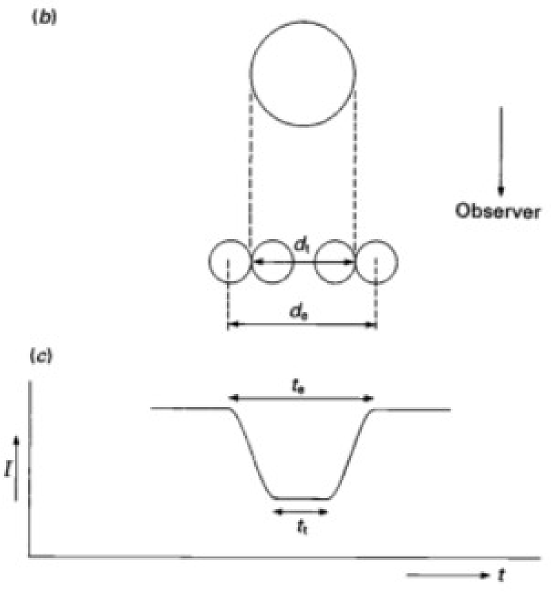

Fig. 9.14. Figure (a) shows the positions of the eclipsing star at first, second, third, and fourth contact as seen from an observer above the plane of the paper. Figure (b) shows the geometry of the eclipse for an observer whose line of sight is in the orbital plane (which is the plane of the paper), not drawn to scale. For a large distance between stars A and B the path of star B can be approximated by a straight line. Figure (c) shows the light curve as a function of time for the duration of the eclipse. During the time t_e star A travels a distance $d_e = 2R_A + 2R_B$. During the time t_t star A travels the distance $d_t = 2R_B - 2R_A$.

Binarias eclipsantes

$$I_{\max} = (\pi R_B^2 \cdot F_B + \pi R_A^2 \cdot F_A)\text{const.}$$

ıe first eclipse the minimum intensity I_1 is given by

$$I_1 = [(\pi R_B^2 - \pi R_A^2)\cdot F_B + \pi R_A^2 \cdot F_A]\text{const.}.$$

the second eclipse the minimum intensity I_2 is giv

$$I_2 = (\pi R_B^2 \cdot F_B)\text{const.}.$$

his we derive

$$I_{\max} - I_2 = (\pi R_A^2 \cdot F_A)\text{const.}$$

$$I_{\max} - I_1 = (\pi R_A^2 \cdot F_B)\text{const.}.$$

$$\frac{I_{\max} - I_2}{I_{\max} - I_1} = \frac{F_A}{F_B}. \qquad (9.25)$$

If we know the flux for one star, we can determine the flux of the other star. Since the radiative fluxes F_A and F_B determine the effective temperatures of the stars we can also determine the ratio of the effective temperatures of the two components of an eclipsing binary system.

$$F_i = \sigma T_i^4$$

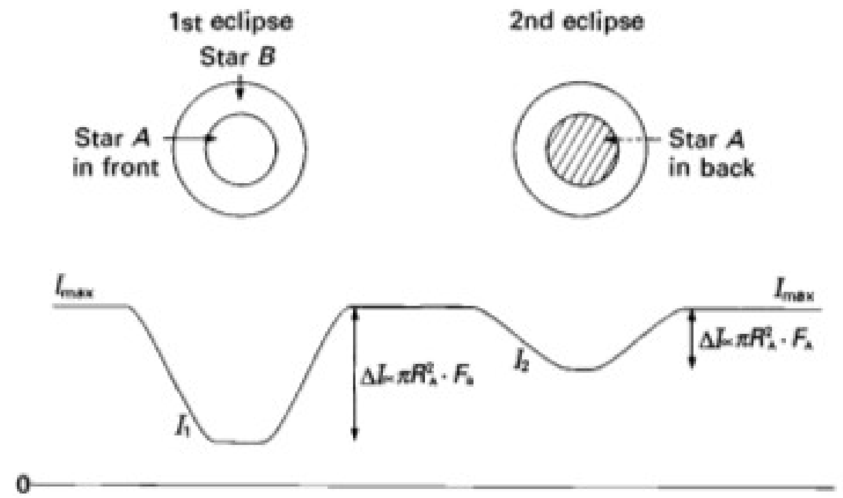

Fig. 9.15. During the first eclipse a fraction of the surface of star B is occulted. During the second eclipse star A is completely covered up. The depths of the light minima depend on the surface fluxes of star A and star B.

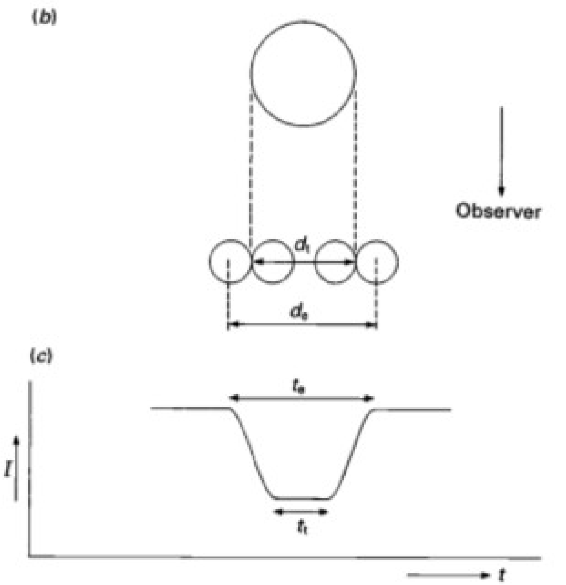

Fig. 9.14. Figure (a) shows the positions of the eclipsing star at first, second, third, and fourth contact as seen from an observer above the plane of the paper. Figure (b) shows the geometry of the eclipse for an observer whose line of sight is in the orbital plane (which is the plane of the paper), not drawn to scale. For a large distance between stars A and B the path of star B can be approximated by a straight line. Figure (c) shows the light curve as a function of time for the duration of the eclipse. During the time t_e star A travels a distance $d_e = 2R_A + 2R_B$. During the time t_t star A travels the distance $d_t = 2R_B - 2R_A$.

Efectos que modifican las curvas de luz

Efecto de elipticidad

Efecto de reflexión entre las componentes

Efecto de oscurecimiento gravitatorio

Efecto de oscurecimiento hacia el limbo

Efectos que modifican las curvas de luz

Efecto de elipticidad

Efecto de reflexión entre las componentes

Efecto de oscurecimiento gravitatorio

Efecto de oscurecimiento hacia el limbo

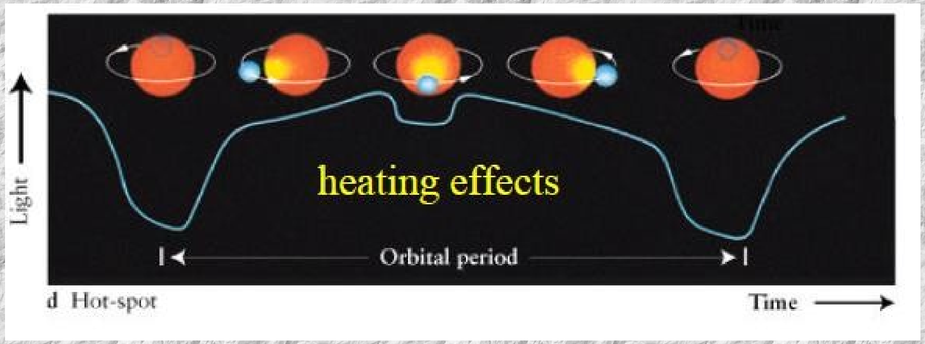

Efectos que modifican las curvas de luz

Efecto de elipticidad

Efecto de reflexión entre las componentes

Efecto de oscurecimiento gravitatorio

Efecto de oscurecimiento hacia el limbo

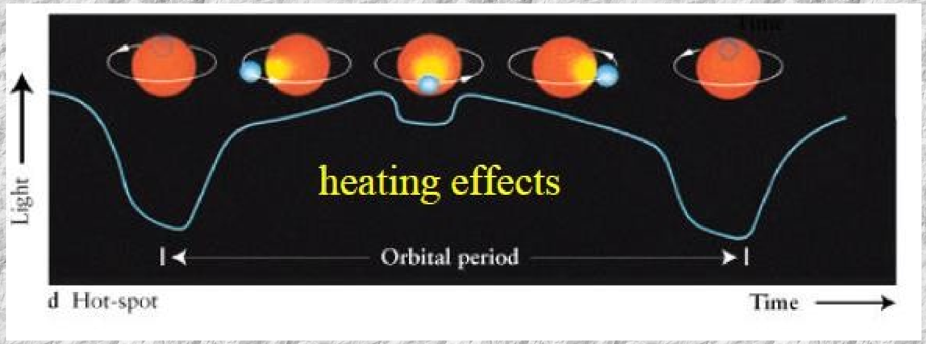

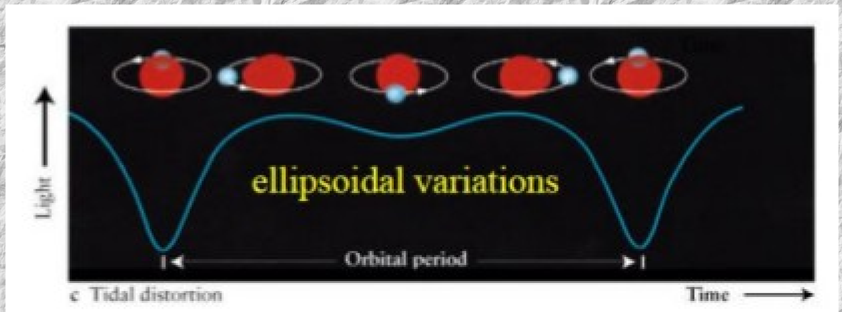

Efectos que modifican las curvas de luz

Efecto de elipticidad

Efecto de reflexión entre las componentes

Efecto de oscurecimiento gravitatorio

Efecto de oscurecimiento hacia el limbo

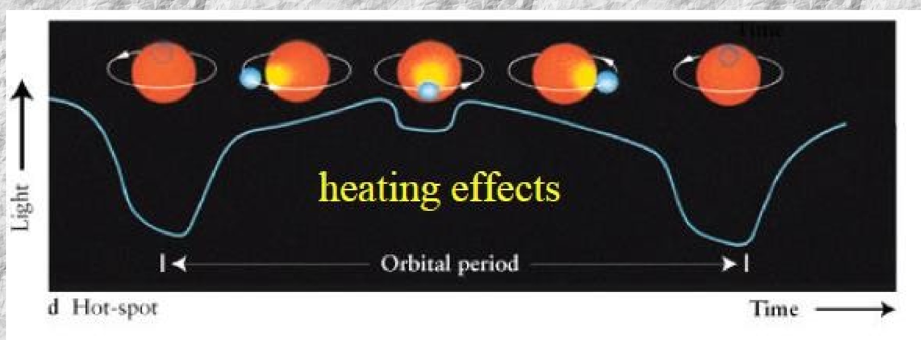

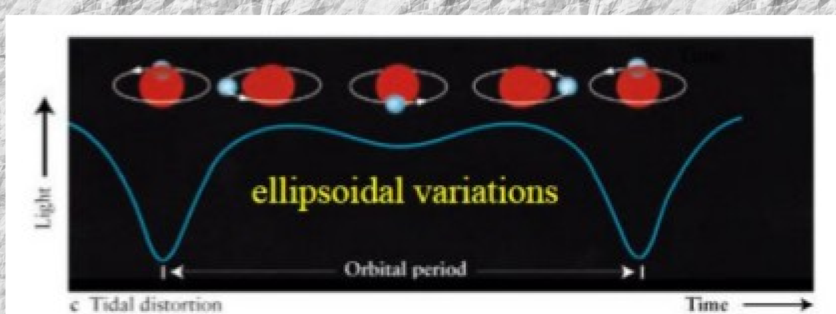

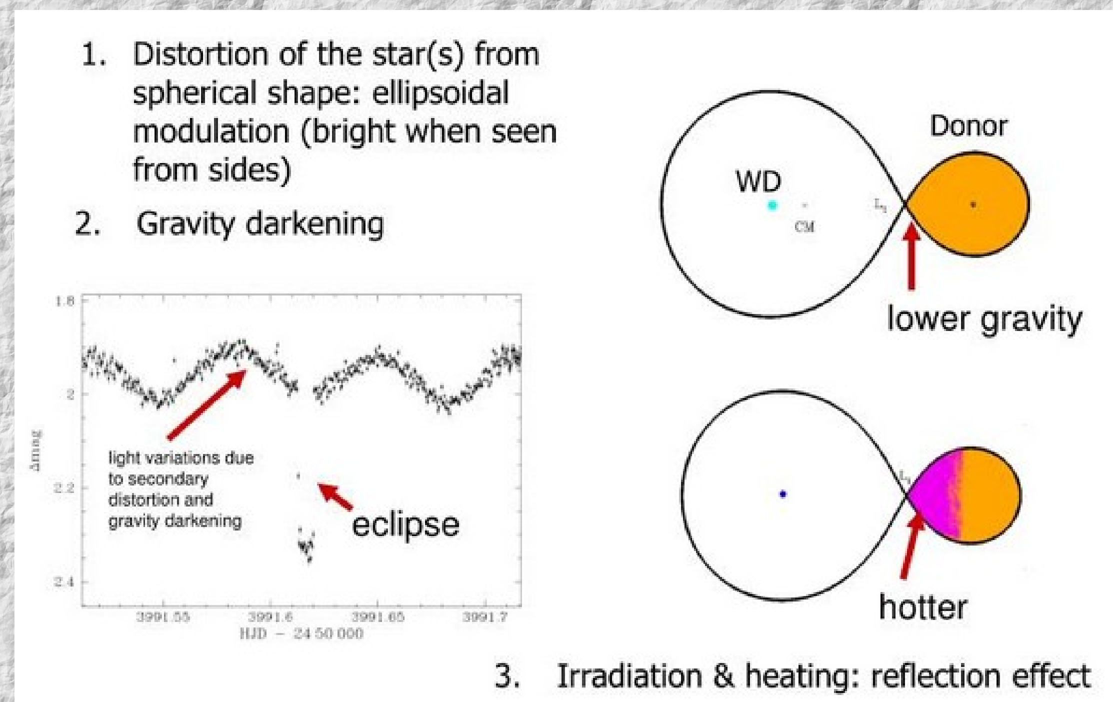

Deformaciones por proximidad de sus componentes

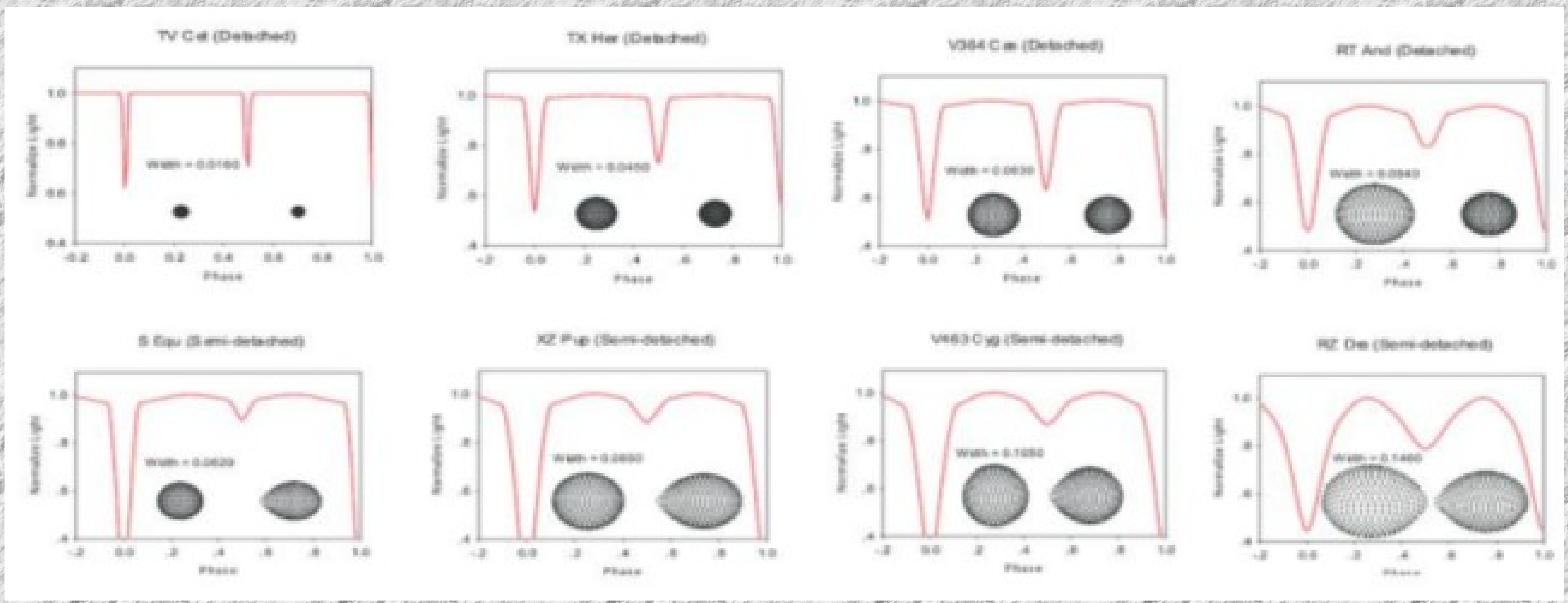

Efecto de oscurecimiento hacia el limbo (depende de long. onda)

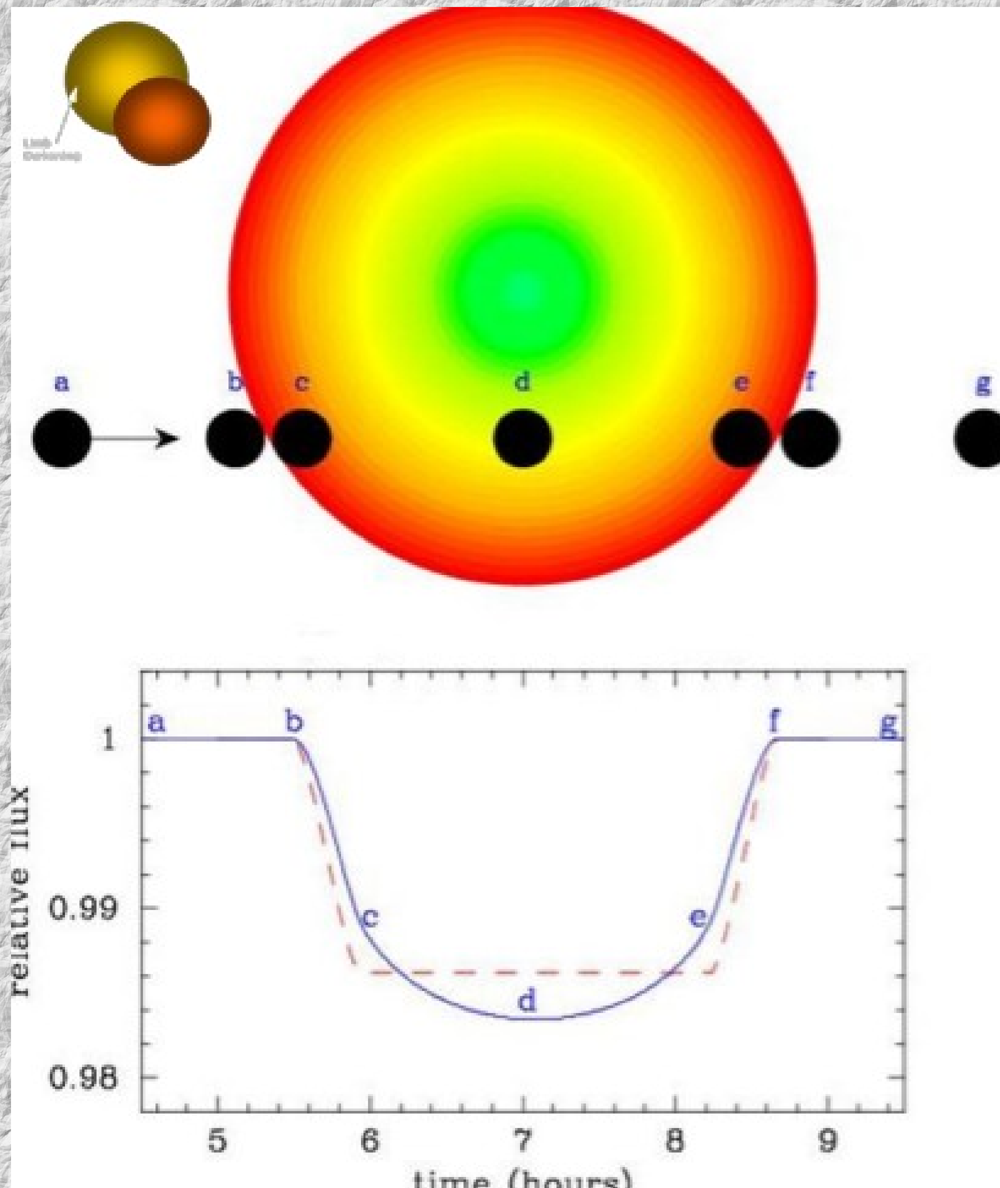

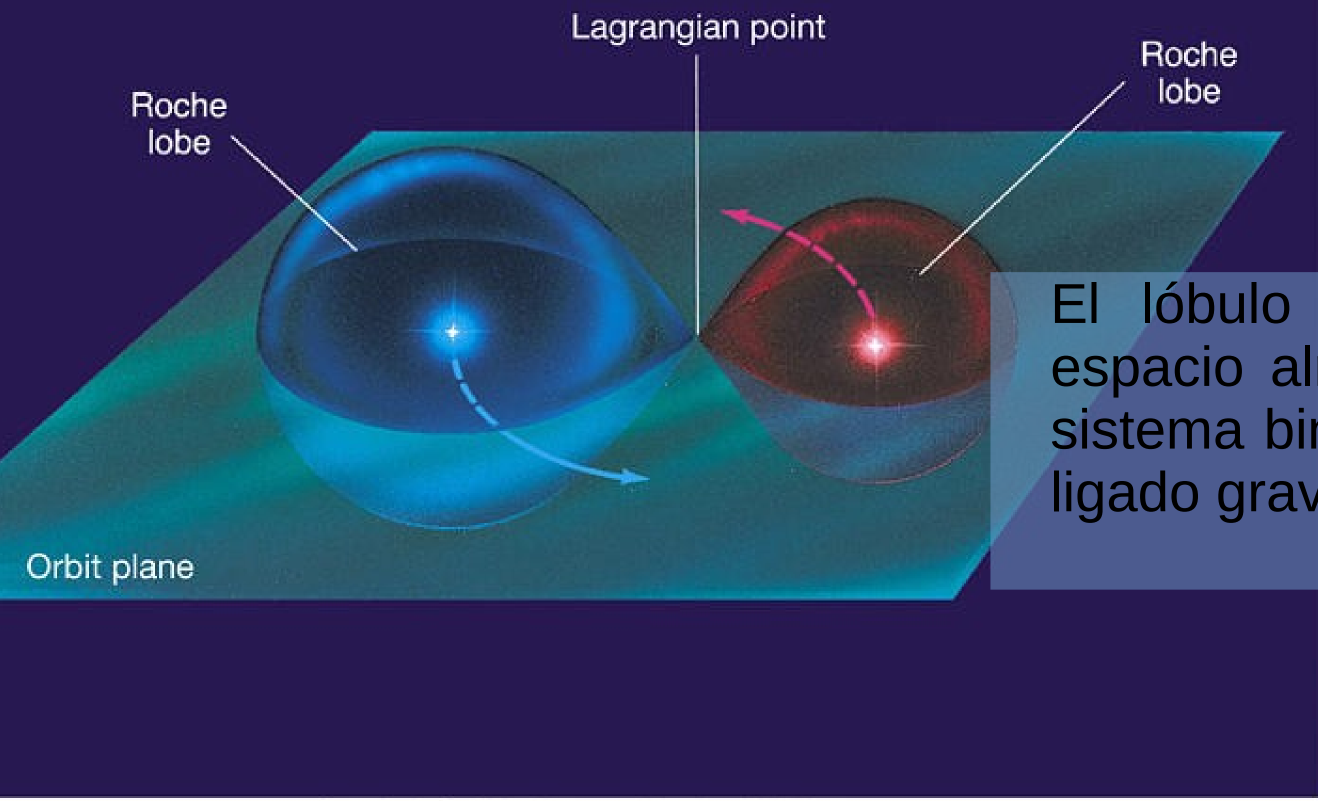

El lóbulo de Roche es la región del espacio alrededor de una estrella en un sistema binario en la que el material está ligado gravitacionalmente a dicha estrella.

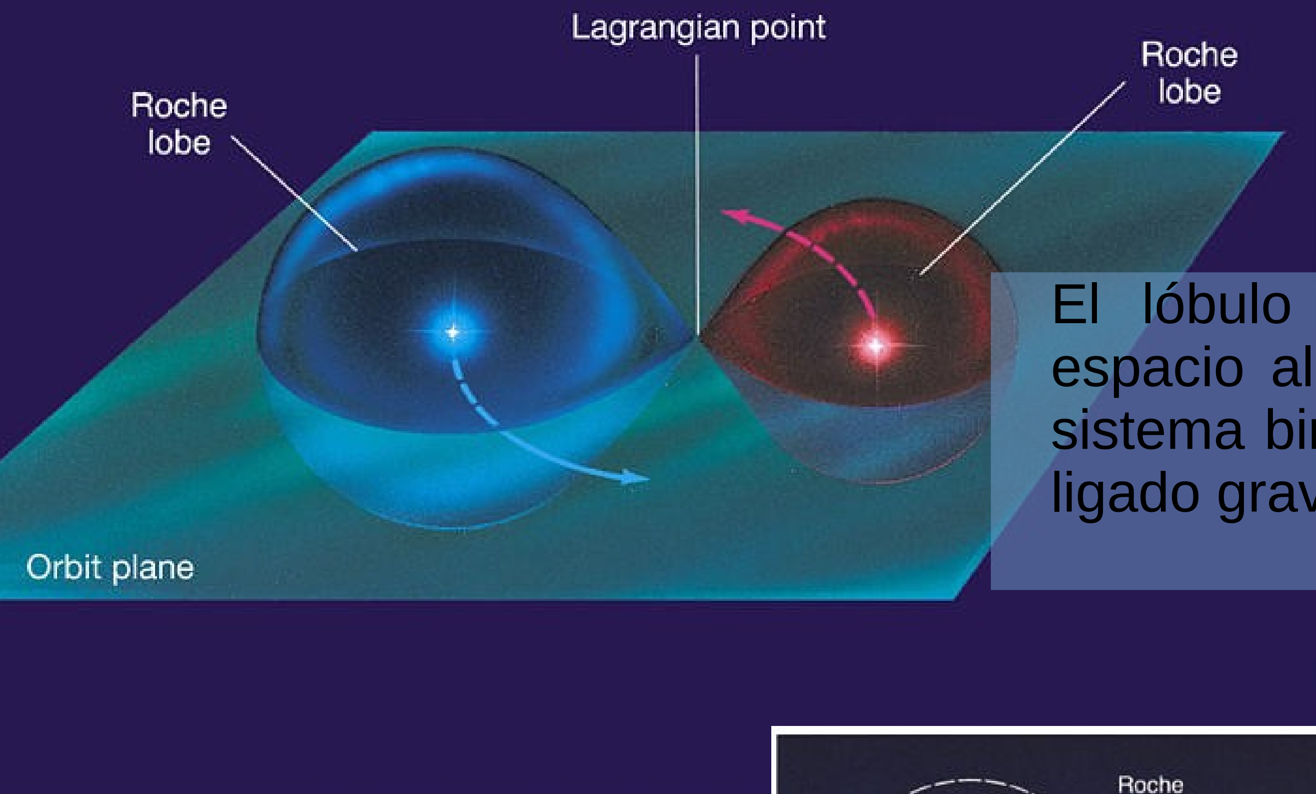

El lóbulo de Roche es la región del espacio alrededor de una estrella en un sistema binario en la que el material está ligado gravitacionalmente a dicha estrella.

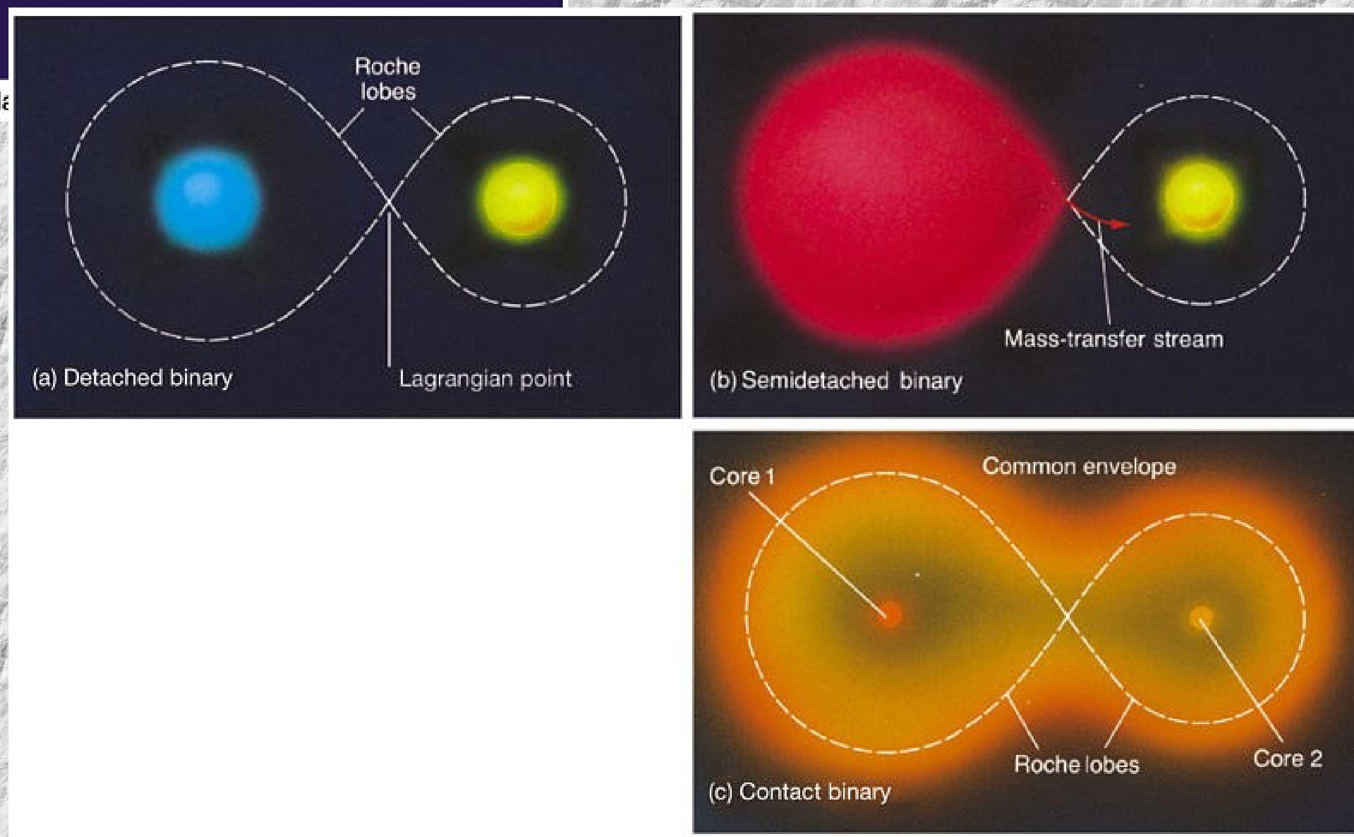

Si la estrella se expande más allá de su lóbulo de Roche entonces el material exterior al lóbulo es atraído por la otra.

Detached Binary

Neither star fills its Roche lobe. Mass transfer unlikely except through strong winds.

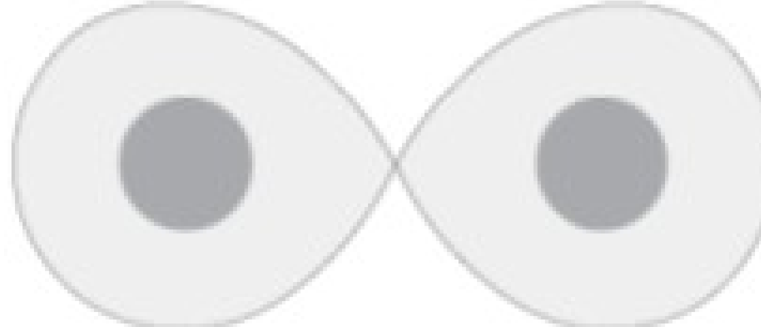

Semidetached Binary

One star fills its Roche lobe; the other does not. Mass transfer can occur throught the L_1 point.

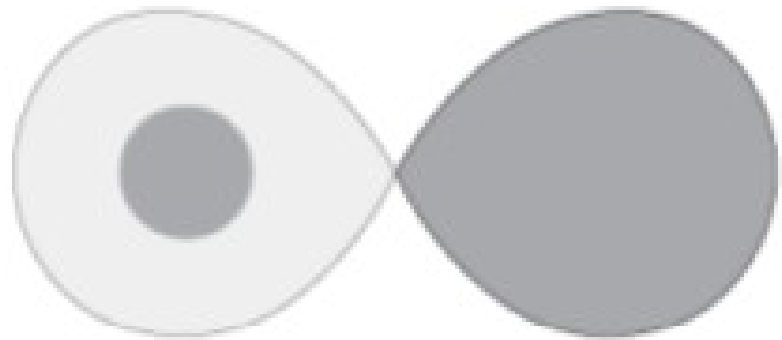

Contact Binary

Each star fills or even overfills its Roche lobe. The two stars may revolve within a common envelope.

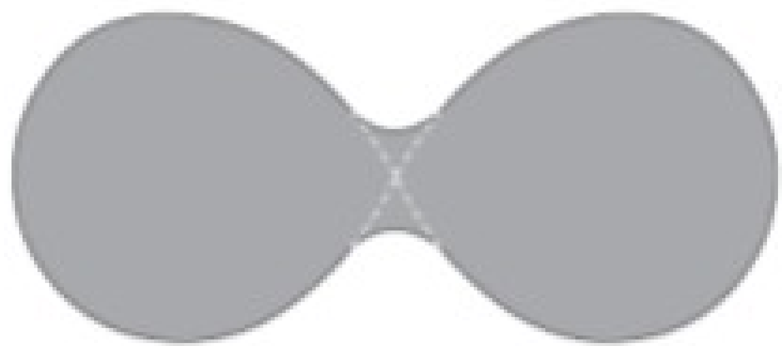

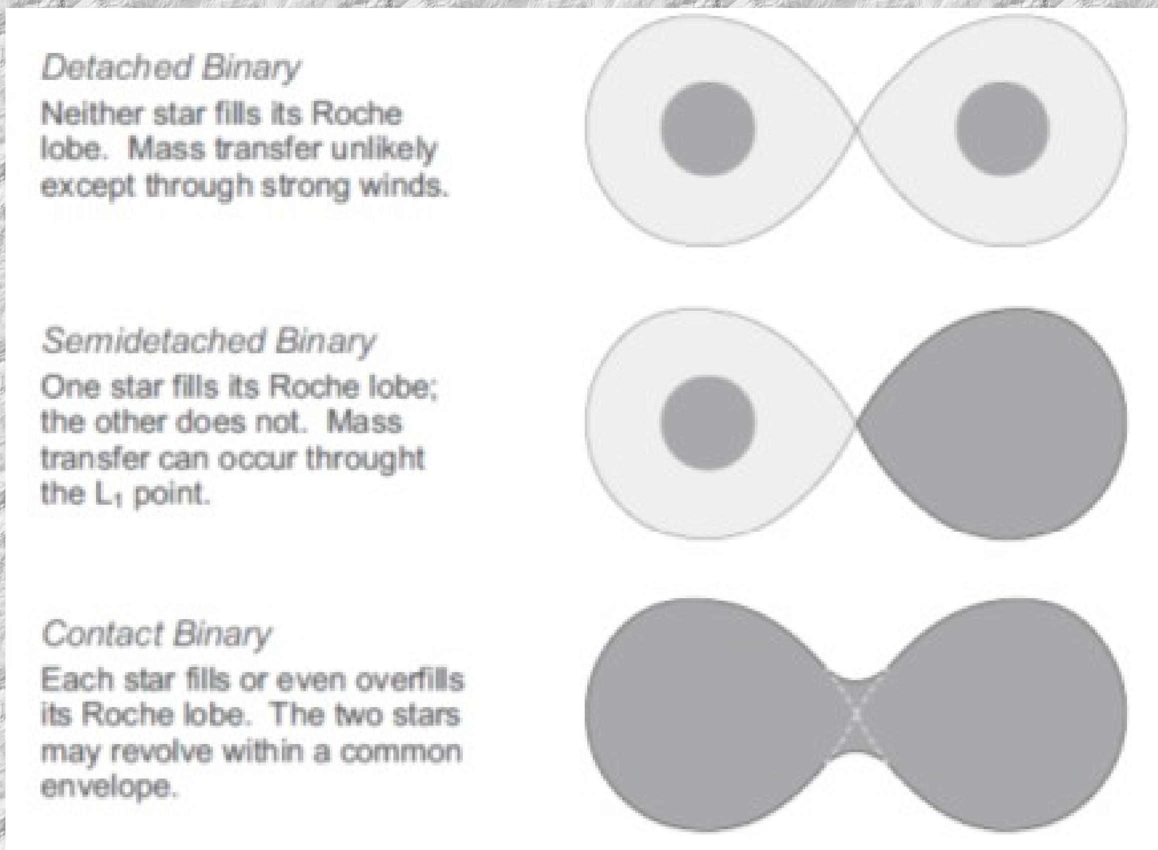
Detached Binary
Neither star fills its Roche lobe. Mass transfer unlikely except through strong winds.
Semidetached Binary
One star fills its Roche lobe; the other does not. Mass transfer can occur throught the L1 point.
Contact Binary
Each star fills or even overfills its Roche lobe. The two stars may revolve within a common envelope.

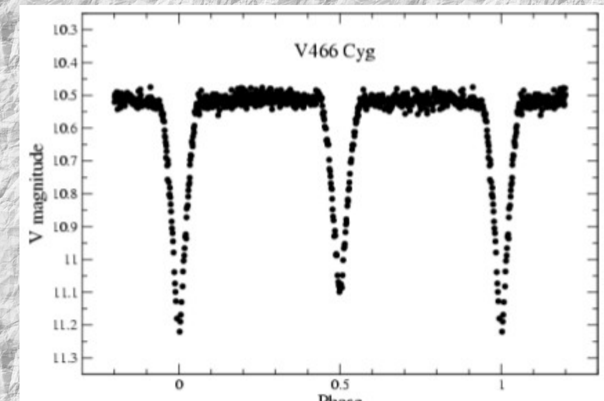
V466 Cyg
V magnitude
10.3
10.4
10.5
10.6
10.7
10.8
10.9
11
11.1
11.2
11.3
0
0.5
1

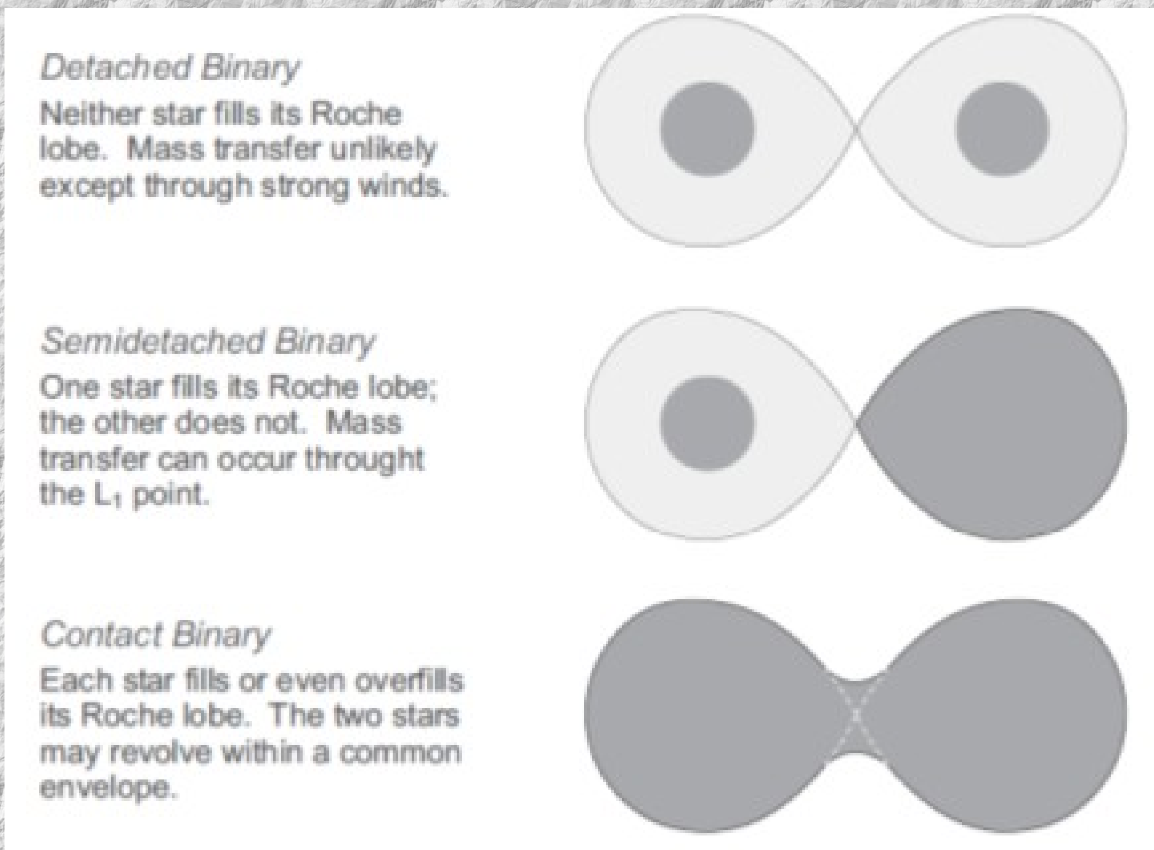
Detached Binary
Neither star fills its Roche lobe. Mass transfer unlikely except through strong winds.
Semidetached Binary
One star fills its Roche lobe; the other does not. Mass transfer can occur throught the L1 point.
Contact Binary
Each star fills or even overfills its Roche lobe. The two stars may revolve within a common envelope.

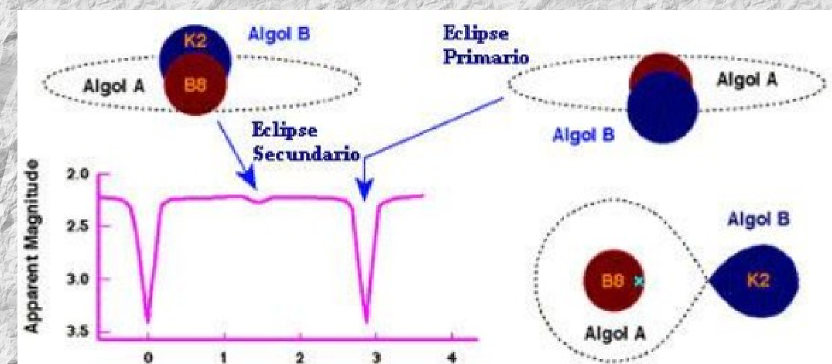
K2
B8
Algol B
Algol A
Eclipse Primario
Algol A
Algol B
Eclipse Secundario
Apparent Magnitude
2.0
2.5
3.0
3.5
0
1
2
3
4
Algol B
B8
K2
Algol A

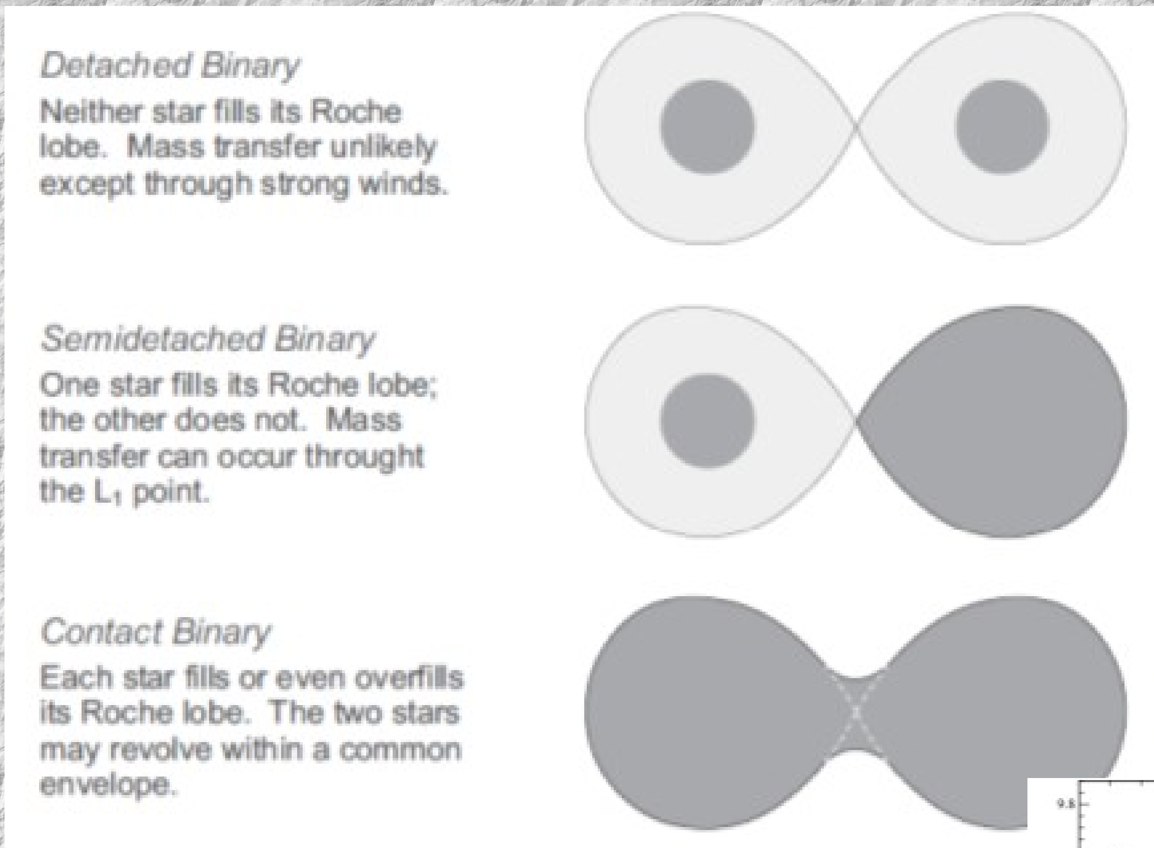
Detached Binary
Neither star fills its Roche lobe. Mass transfer unlikely except through strong winds.
Semidetached Binary
One star fills its Roche lobe; the other does not. Mass transfer can occur throught the L1 point.
Contact Binary
Each star fills or even overfills its Roche lobe. The two stars may revolve within a common envelope.

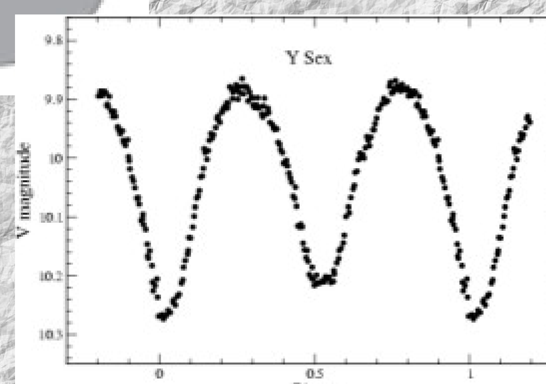
Y Sex
V magnitude
9.8
9.9
10
10.1
10.2
10.3
0
0.5
1
Phase


Crédito:
Imagen: ESO/M.-R. Cioni/VISTA Magellanic Cloud survey. Agradecimiento: Cambridge Astronomical Survey Unit.
Ilustración: ESO/L. Calçada.
Estrella doble gigante VFTS 352

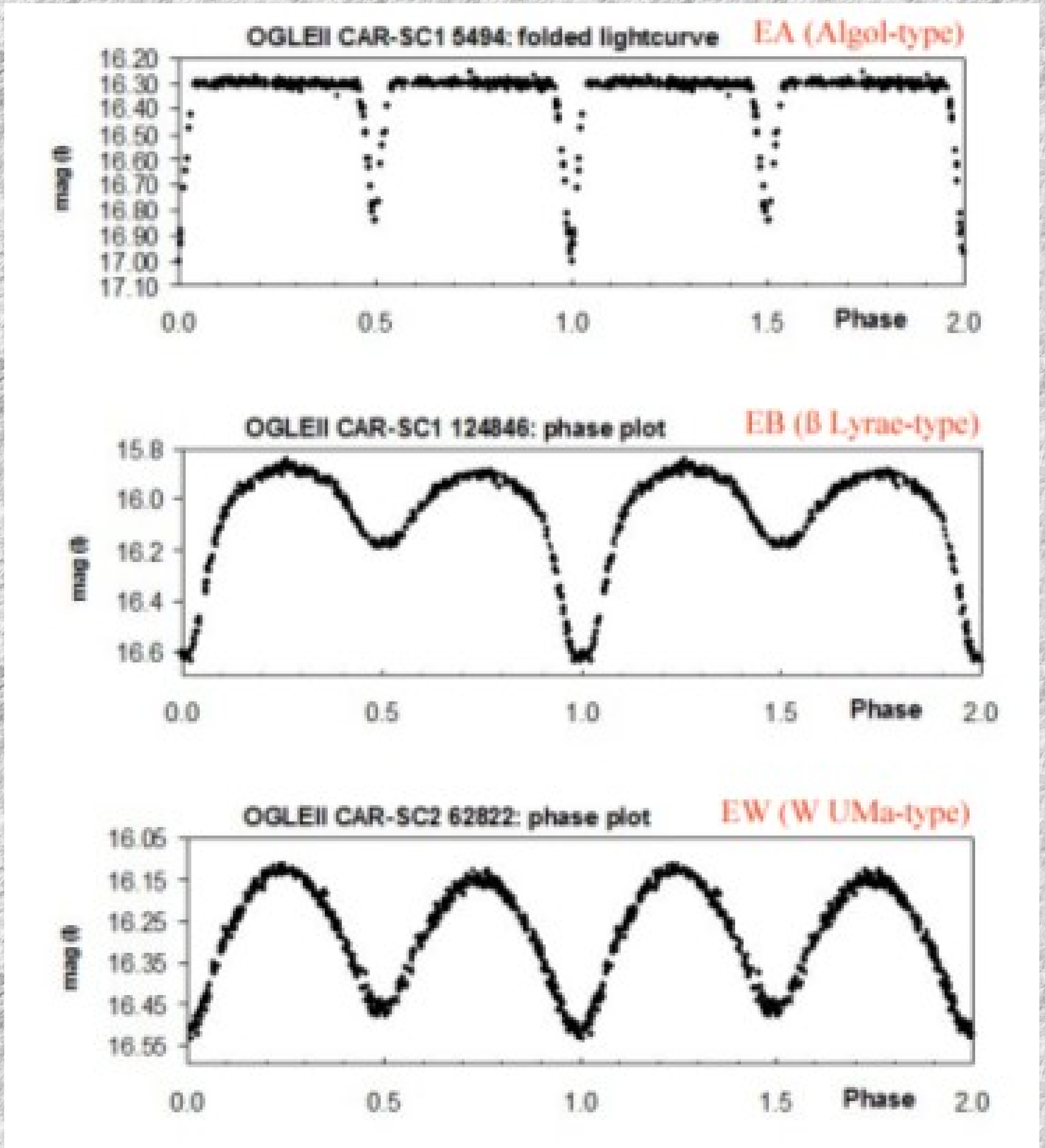
OGLEII CAR-SC1 5494: folded lightcurve
EA (Algol-type)
mag (I)
Phase
OGLEII CAR-SC1 124846: phase plot
EB (β Lyrae-type)
mag (I)
Phase
OGLEII CAR-SC2 62822: phase plot
EW (W UMa-type)
mag (I)
Phase

Binarias espectroscópicas (efecto Doppler)

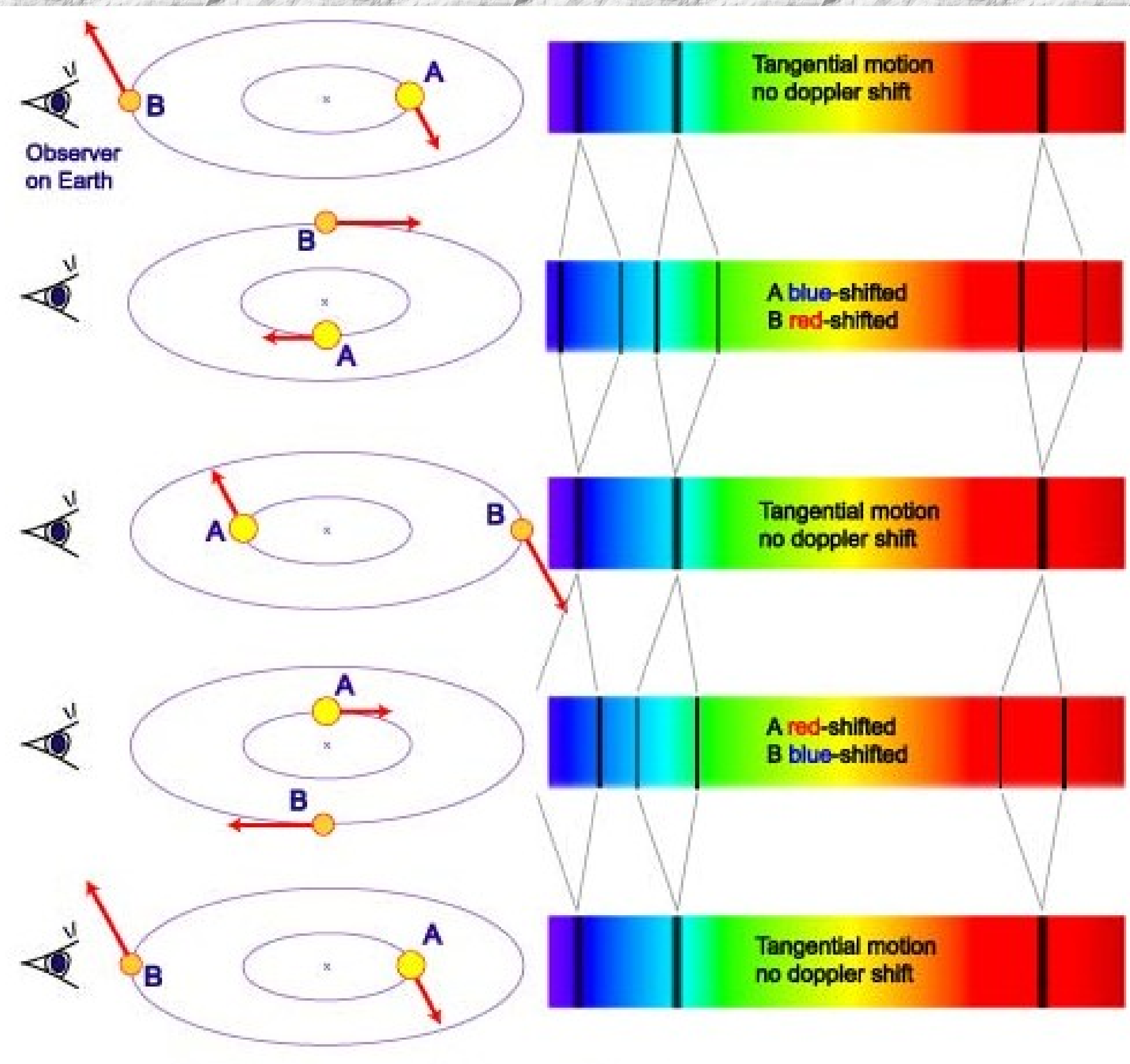

La estrella más masiva A y la estrellas menos masiva B, orbitan alrededor del CM del sistema. El espectro observado muestra líneas espectrales con componentes dobles y desplazamientos de las líneas con relación a la posición de reposo.
El del desplazamiento depende del grado de alineamiento con el observador y la velocidad orbital de la estrella.

$$\frac{\Delta\lambda}{\lambda_0} = \frac{v_r}{c},$$

Binarias espectroscópicas

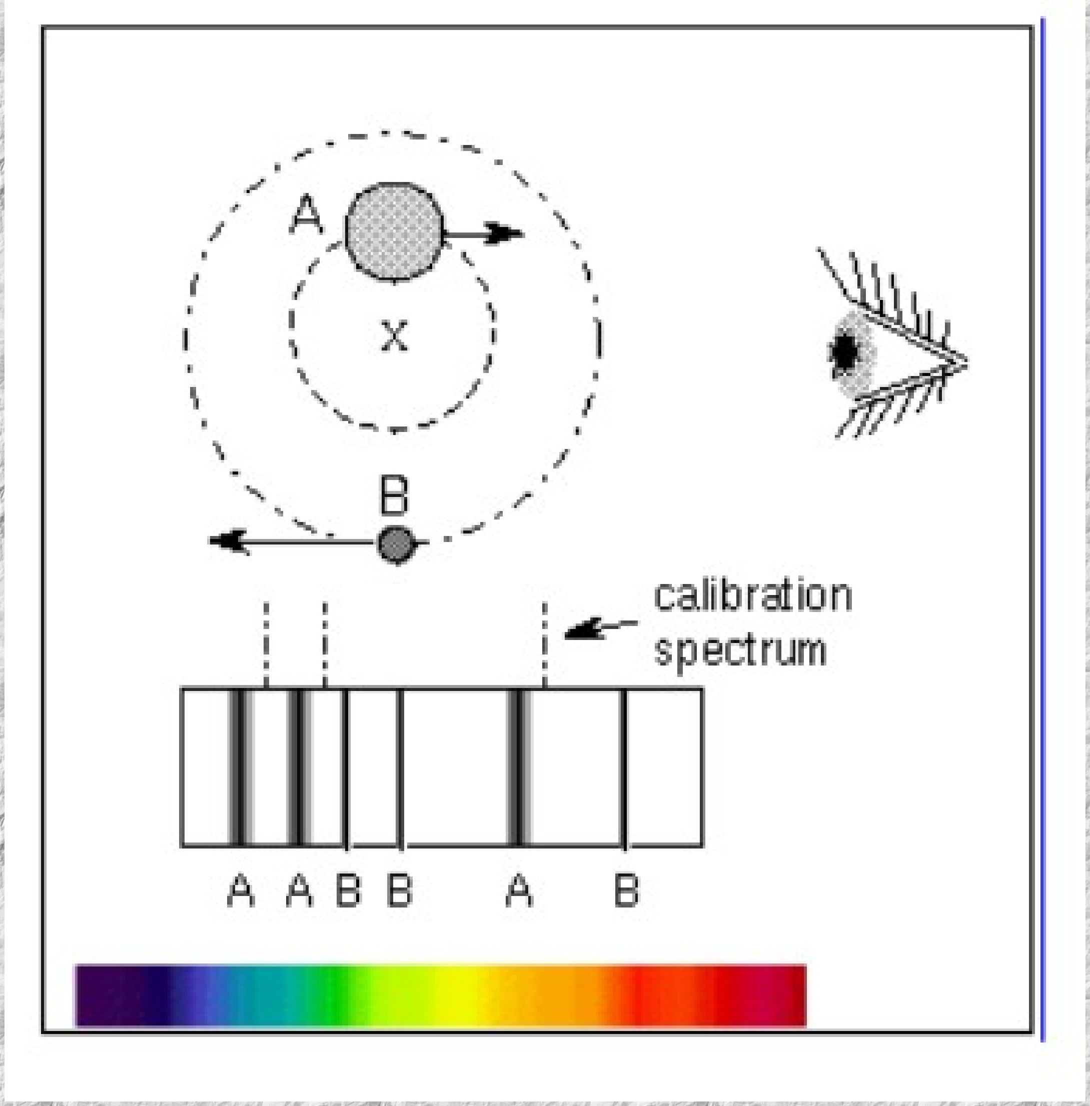

Binarias espectroscópicas

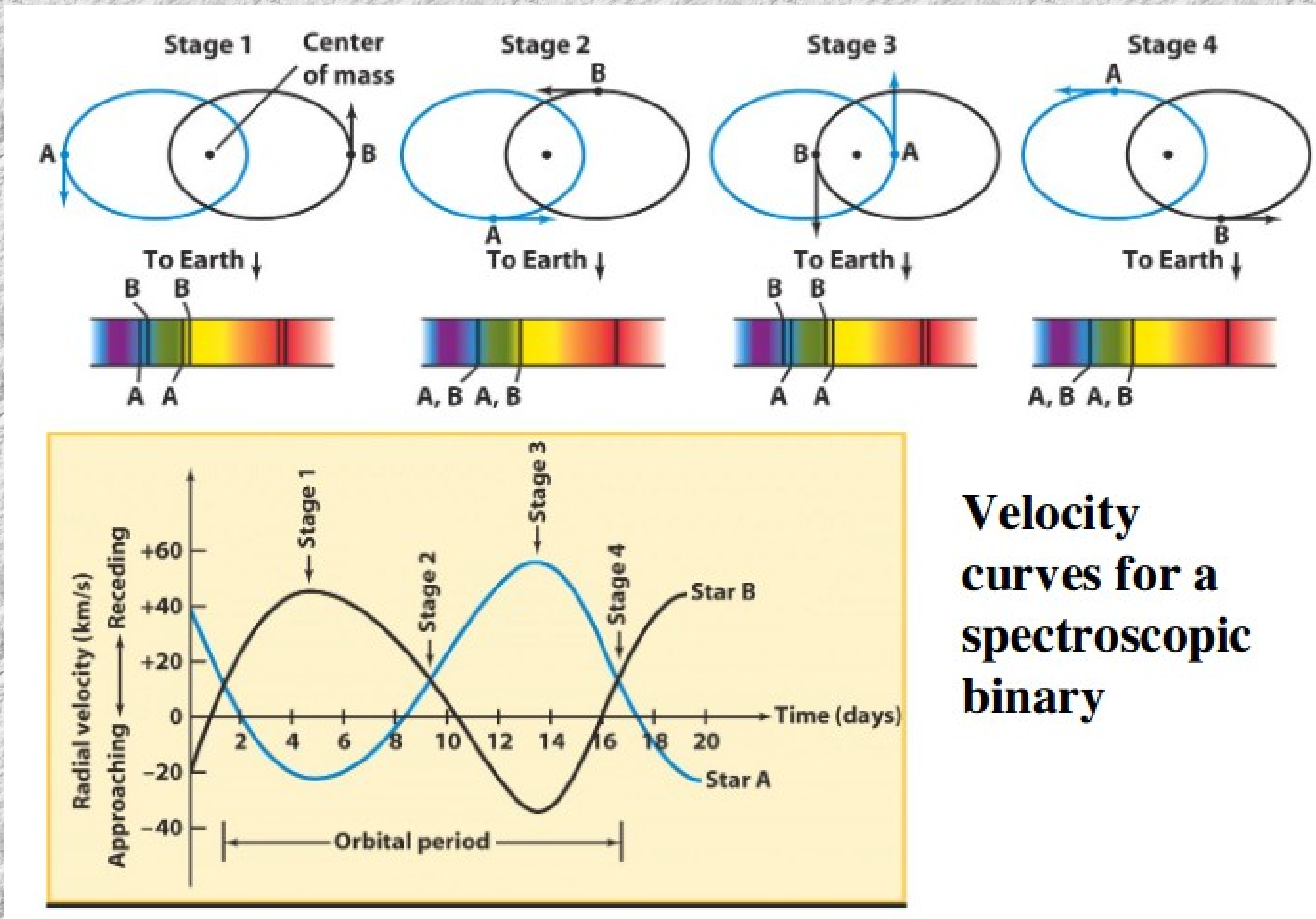

Binarias espectroscópicas (con dos espectros)

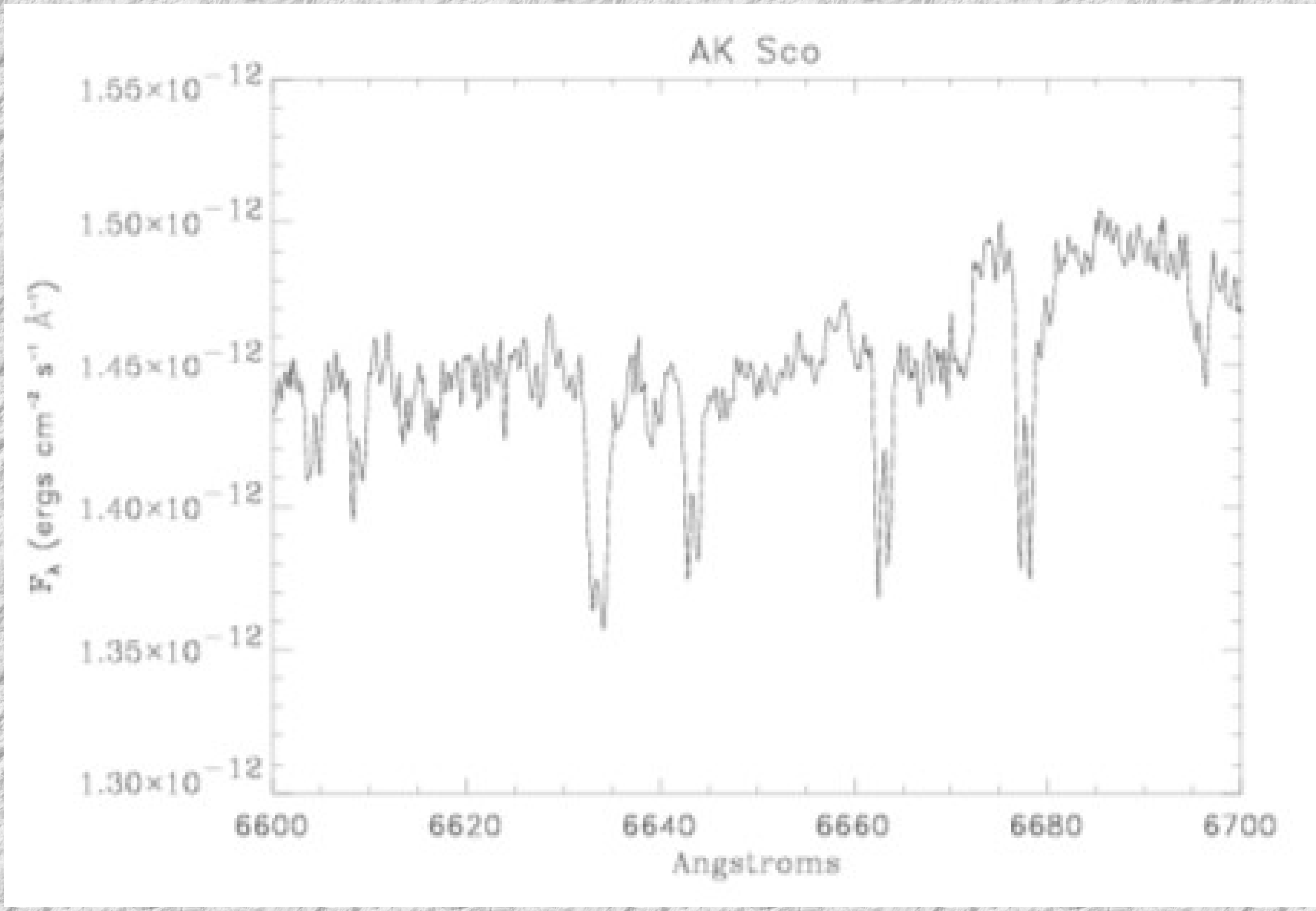

Binarias espectroscópicas (con un solo espectro)

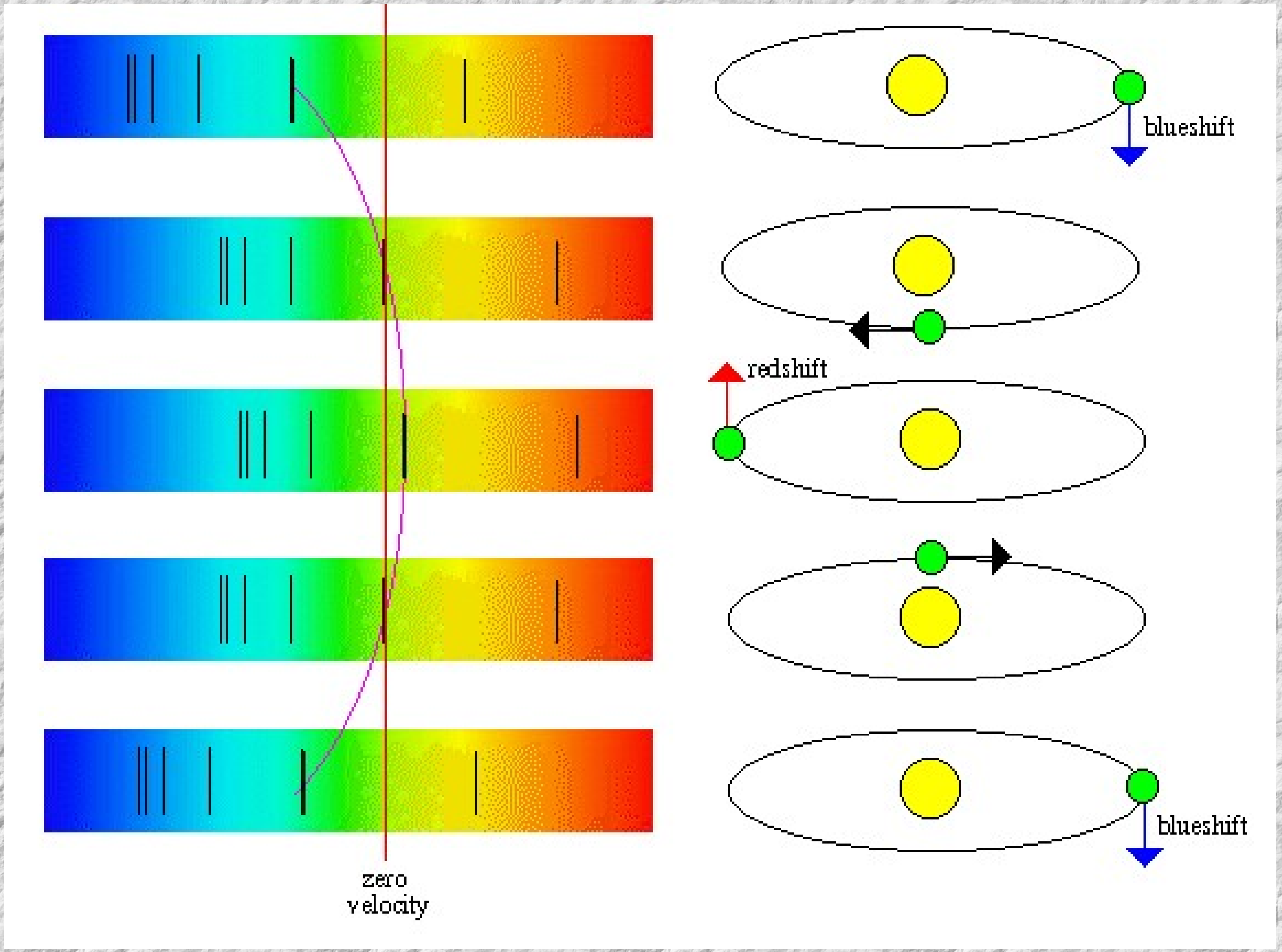

Se observa evidencia del movimiento orbital (desplazamiento Doppler de las líneas espectrales) de la componente más luminosa

Binarias espectroscópicas
Velocidades radiales

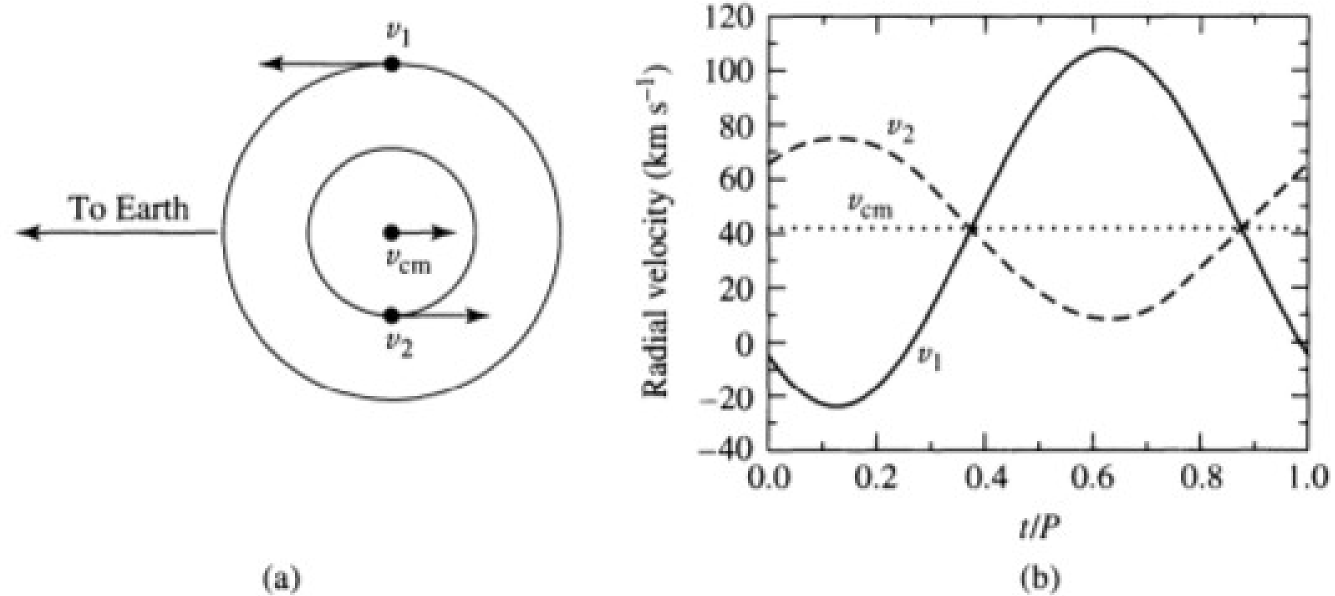

FIGURE 7.5 The orbital paths and radial velocities of two stars in circular orbits ($e = 0$). In this example, $M_1 = 1\ M_\odot$, $M_2 = 2\ M_\odot$, the orbital period is $P = 30$ d, and the radial velocity of the center of mass is $v_{cm} = 42$ km s^{-1}. v_1, v_2, and v_{cm} are the velocities of Star 1, Star 2, and the center of mass, respectively. (a) The plane of the circular orbits lies along the line of sight of the observer. (b) The observed radial velocity curves.

Binarias espectroscópicas Velocidades radiales

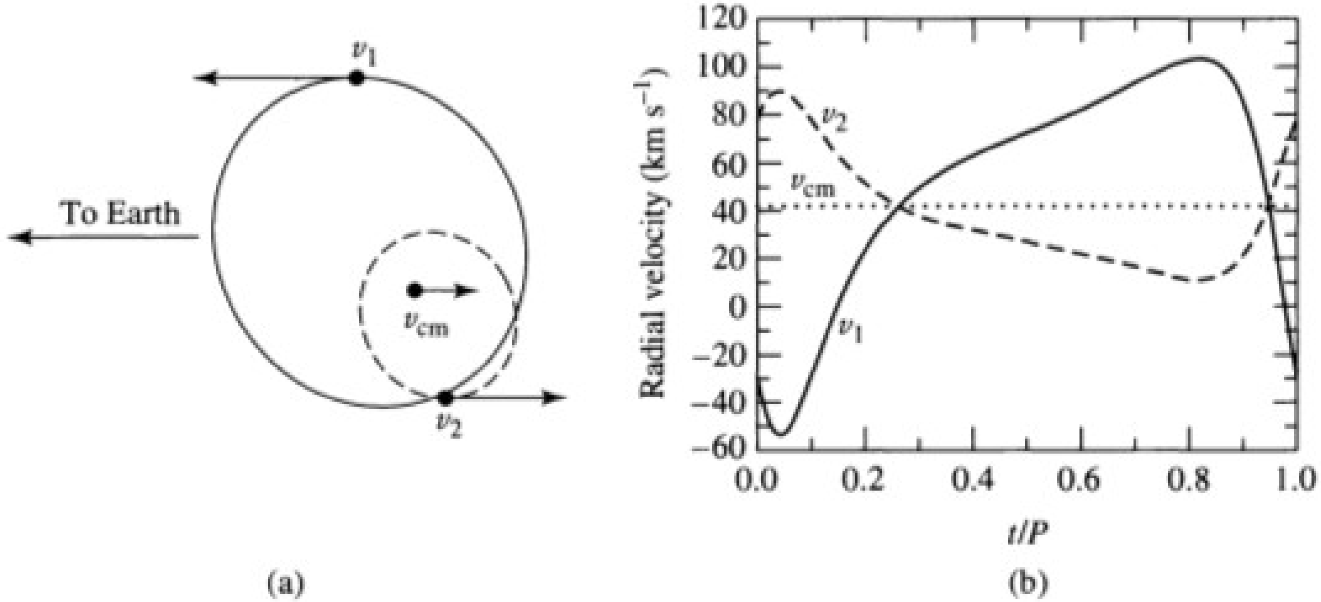

FIGURE 7.6 The orbital paths and radial velocities of two stars in elliptical orbits ($e = 0.4$). As in Fig. 7.5, $M_1 = 1\ M_\odot$, $M_2 = 2\ M_\odot$, the orbital period is $P = 30$ d, and the radial velocity of the center of mass is $v_{cm} = 42$ km s^{-1}. In addition, the orientation of periastron is 45°. v_1, v_2, and v_{cm} are the velocities of Star 1, Star 2, and the center of mass, respectively. (a) The plane of the orbits lies along the line of sight of the observer. (b) The observed radial velocity curves.

Velocidad del sistema (centro de masa)

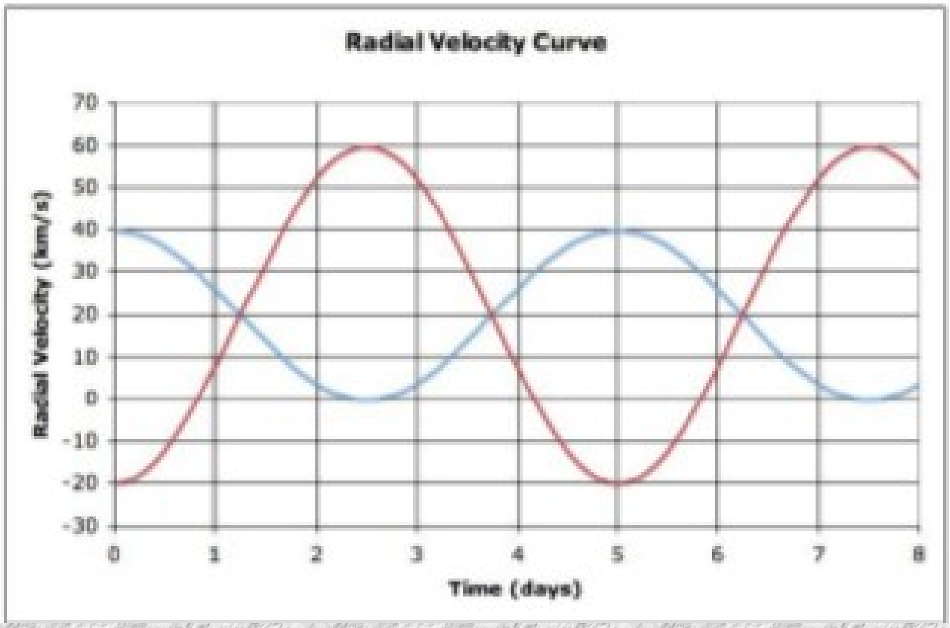

En el caso de dos espectros visibles, la V_{cm} resulta el valor alrededor de cual ambas curvas de velocidad radial tiene igual amplitud.

Velocidad del sistema (centro de masa)

Vr = V_CM + Vo → Vo = velocidad de la estrella en la órbita absoluta
- La estrella se mueve en una órbita elíptica alrededor del CM
- Como **la distancia que se mueve la estrella desde y hacia el Sol** se encuentra **integrando la velocidad en el intervalo de tiempo apropiado,** ***V_CM se obtiene trazando la línea recta que deja igual área por encima y por debajo de ella***.

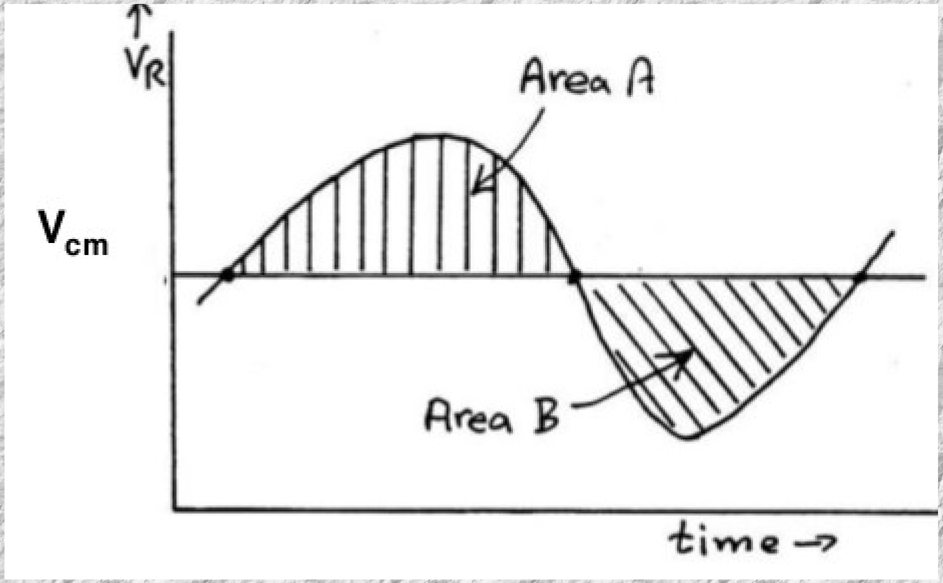

Curva de velocidades radiales

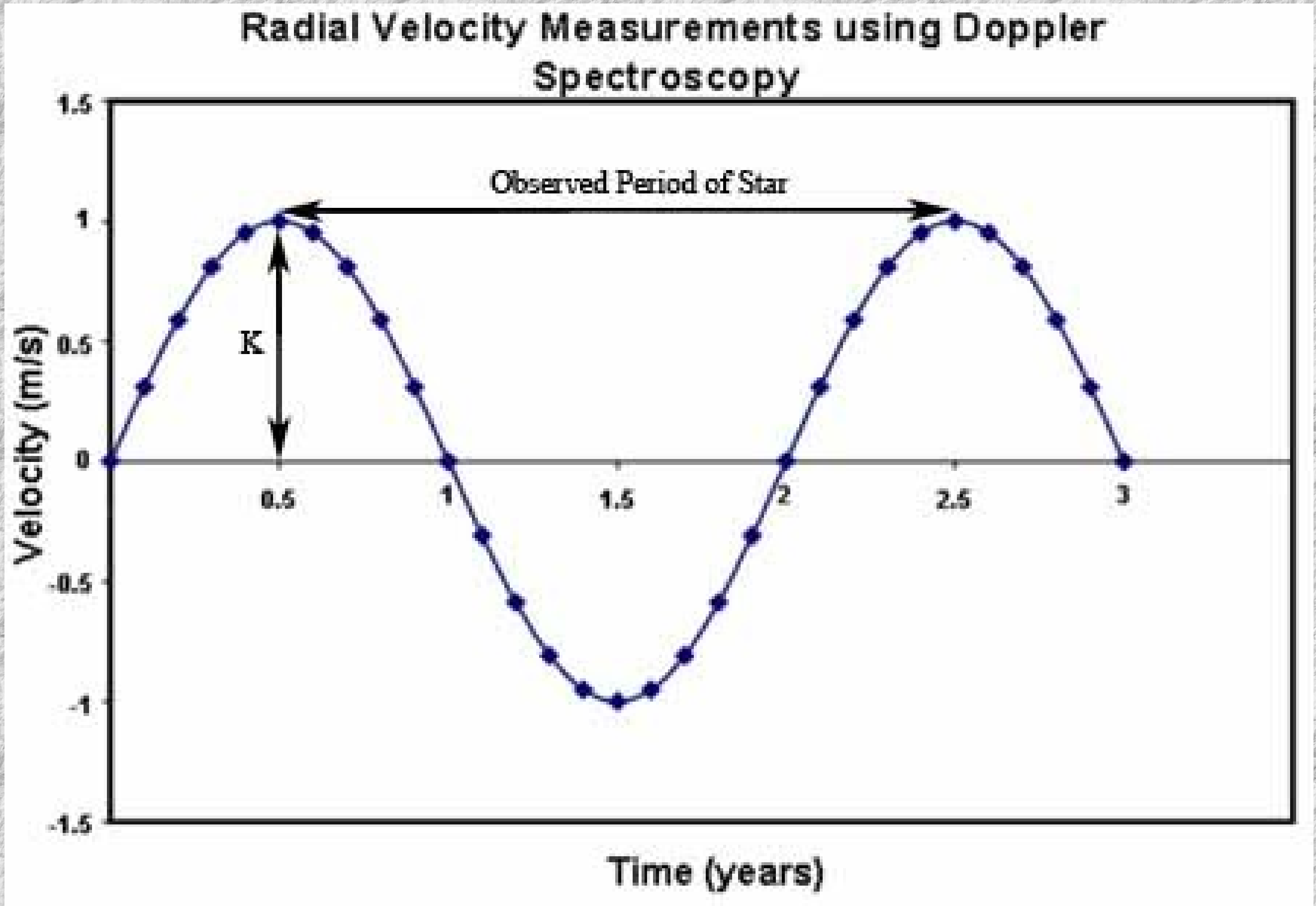

$$\boxed{V_{r,1} = V_0 + K_1[e\cos\omega + \cos(\nu + \omega)]}$$

$$K_1 = \frac{2\pi}{P}\frac{a_1 \operatorname{sen} i}{\sqrt{1-e^2}}$$

Curva de velocidades radiales

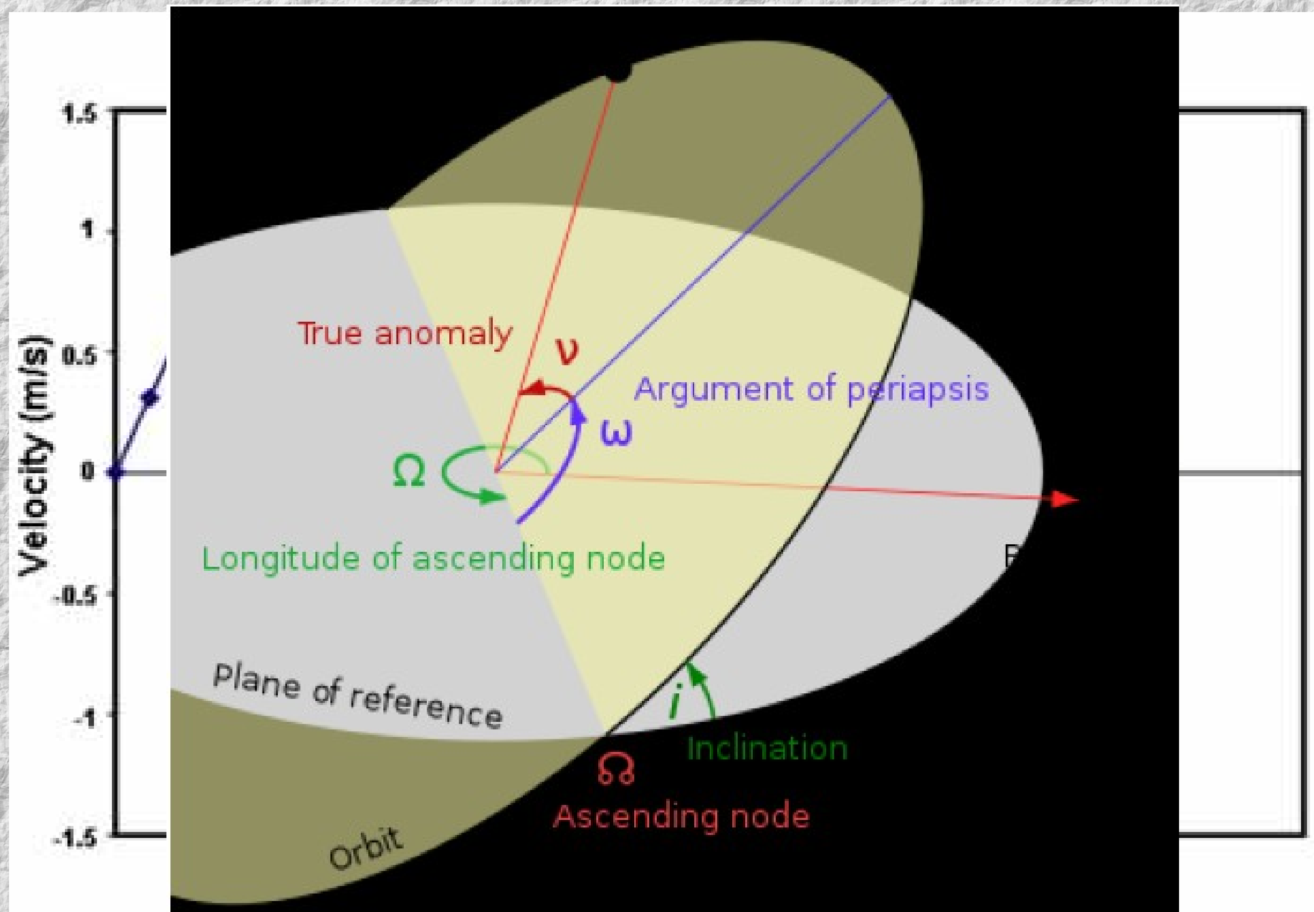

$$\boxed{V_{r,1} = V_0 + K_1[e\cos\omega + \cos(\nu + \omega)]}$$

$$K_1 = \frac{2\pi}{P}\frac{a_1 \operatorname{sen} i}{\sqrt{1-e^2}}$$

Curva de velocidades radiales

$$\boxed{V_{r,1} = V_0 + K_1[e\cos\omega + \cos(\nu + \omega)]}$$

$$K_1 = \frac{2\pi}{P}\frac{a_1 \operatorname{sen} i}{\sqrt{1-e^2}}$$

Si *i* = 90° y *e* = 0 → K_i = 2 (“pi”) a_i / P

→ K_1/K_2 2 = a_1/a_2

Como a = $a_1 + a_2$ y $m_1a_1 = m_2a_2$

→ $(m_1+m_2) = a^3 / P^2$

Mido masas de las estrellas!!!!

Sea la órbita elíptica, con el plano orbital perpendicular al plano del cielo (i = 90°).

Las veloci soidales y
dependen cto al
observado

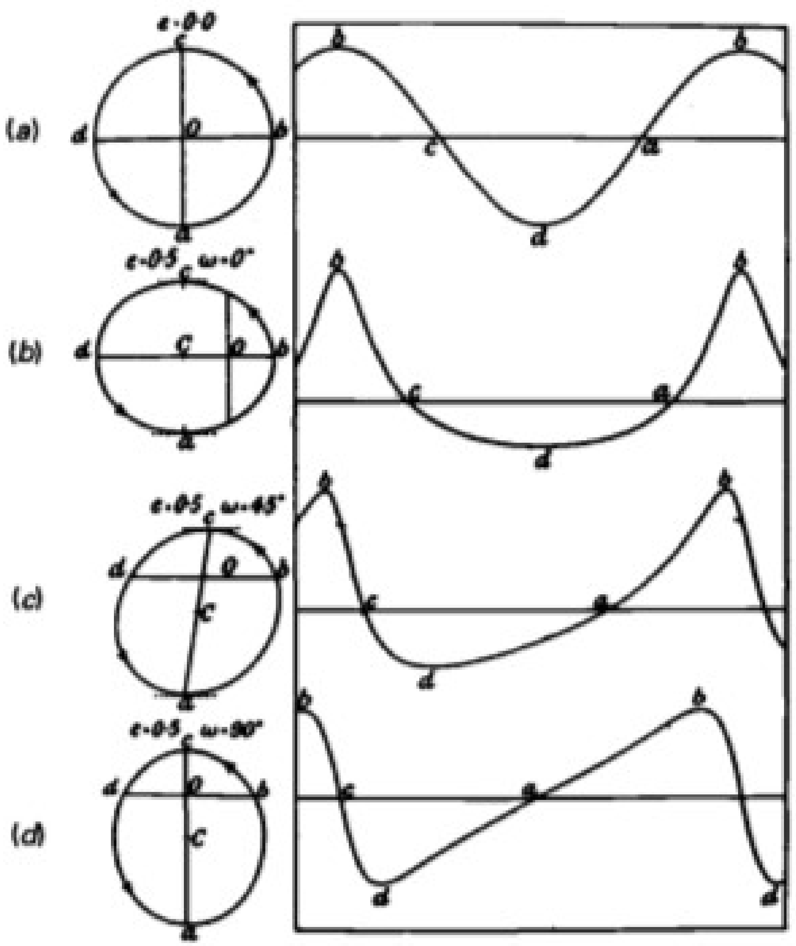

Fig. 9.8. Plotted are radial velocity curves to be seen for stellar orbits with zero ellipticities (*a*) and with an ellipticity $e = 0.5$ for $\omega = 0$ (*b*), and for the same ellipticity but $\omega = 45°$ (*c*), and also for $\omega = 90°$ (*d*). $e \neq 0$ generally introduces a difference between maximum positive and negative velocities (see (*c*) and (*d*)) except in the case when $\omega = 90°$. In this case the time difference between points *b* and *d* on the one side and between points *d* and *b* on the other side (d) gives a measure of the ellipticity. (From Becker 1950.)

Sea la órbita elíptica, con el plano orbital perpendicular al plano del cielo (i = 90°).

Las velocidades radiales observadas no son sinusoidales y dependen de la orientación de la órbita con respecto al observador (de ω, argumento del periastro)

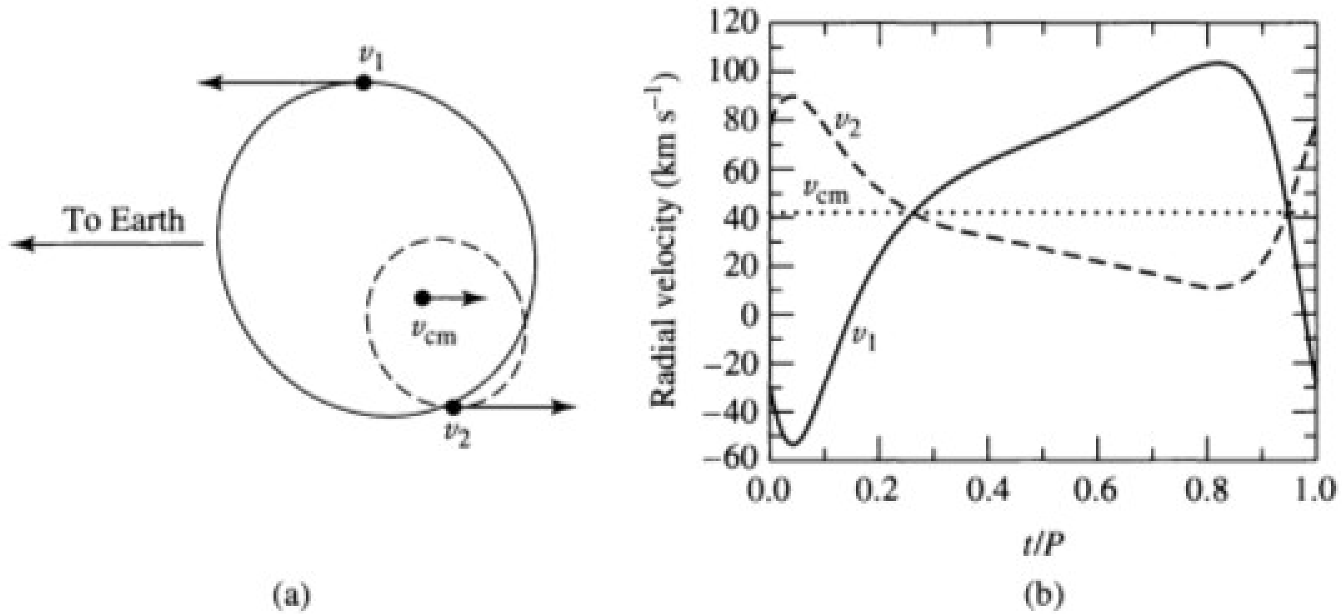

FIGURE 7.6 The orbital paths and radial velocities of two stars in elliptical orbits ($e = 0.4$). As in Fig. 7.5, $M_1 = 1\ M_\odot$, $M_2 = 2\ M_\odot$, the orbital period is $P = 30$ d, and the radial velocity of the center of mass is $v_{cm} = 42$ km s^{-1}. In addition, the orientation of periastron is 45°. v_1, v_2, and v_{cm} are the velocities of Star 1, Star 2, and the center of mass, respectively. (a) The plane of the orbits lies along the line of sight of the observer. (b) The observed radial velocity curves.

Función de masa

If we assume that the orbital eccentricity is very small ($e \ll 1$), then the speeds of the stars are essentially constant and given by $v_1 = 2\pi a_1/P$ and $v_2 = 2\pi a_2/P$ for stars of mass m_1 and m_2, respectively, where a_1 and a_2 are the radii (semimajor axes) and P is the period of the orbits. Solving for a_1 and a_2 and substituting into Eq. (7.1), we find that the ratio of the masses of the two stars becomes

$$\frac{m_1}{m_2} = \frac{r_2}{r_1} = \frac{a_2}{a_1}, \longrightarrow \frac{m_1}{m_2} = \frac{v_2}{v_1}. \tag{7.4}$$

Because $v_{1r} = v_1 \sin i$ and $v_{2r} = v_2 \sin i$, Eq. (7.4) can be written in terms of the observed radial velocities rather than actual orbital velocities:

$$\boxed{\frac{m_1}{m_2} = \frac{v_{2r}/\sin i}{v_{1r}/\sin i} = \frac{v_{2r}}{v_{1r}}.} \tag{7.5}$$

Función de masa

If we assume that the orbital eccentricity is very small ($e \ll 1$), then the speeds of the stars are essentially constant and given by $v_1 = 2\pi a_1/P$ and $v_2 = 2\pi a_2/P$ for stars of mass m_1 and m_2, respectively, where a_1 and a_2 are the radii (semimajor axes) and P is the period of the orbits. Solving for a_1 and a_2 and substituting into Eq. (7.1), we find that the ratio of the masses of the two stars becomes

$$\frac{m_1}{m_2} = \frac{r_2}{r_1} = \frac{a_2}{a_1}, \quad \longrightarrow \quad \frac{m_1}{m_2} = \frac{v_2}{v_1}. \tag{7.4}$$

Because $v_{1r} = v_1 \sin i$ and $v_{2r} = v_2 \sin i$, Eq. (7.4) can be written in terms of the observed radial velocities rather than actual orbital velocities:

$$\boxed{\frac{m_1}{m_2} = \frac{v_{2r}/\sin i}{v_{1r}/\sin i} = \frac{v_{2r}}{v_{1r}}.} \tag{7.5}$$

In the ratio the $\sin i$ factor cancels out. But if we want to determine the mass sum we are in trouble. We know that $r_1 = v_1 P/(2\pi)$ and similarly $r_2 = v_2 P/(2\pi)$. Since we only know $v_1 \sin i$ and $v_2 \sin i$ we also can only determine $r_1 \sin i$ and $r_2 \sin i$. According to (9.8) we therefore can determine only

$$\longrightarrow \quad (M_1 + M_2)\sin^3 i = \frac{(r_1 + r_2)^3 \sin^3 i}{P^2}\frac{4\pi^2}{G}. \tag{9.26}$$

The mass sum remains uncertain by the factor $\sin^3 i$, and therefore both masses remain uncertain by the same factor.

Binarias espectro-fotométricas (dos espectros + curva de luz)

→ masas y radios de cada estrella

De las dos curvas de velocidades radiales obtengo:

$M_1 \sin^3 i$ y $M_2 \sin^3 i$

$a_1 \sin i$ y $a_2 \sin i$ luego tengo: $a \operatorname{sen} i$

De la curva de luz obtengo:

R_1/a y R_2/a además de i

Luego puedo determinar M_1, M_2, R_1, R_2,

The Astronomical Journal, 133:255–260, 2007 January

LIGHT-CURVE AND RADIAL VELOCITY STUDY OF THE CONTACT BINARY BD +42 2782

Wenxian Lu,[1] Bruce J. Hrivnak, and Bradley W. Rush[1,2]
Department of Physics and Astronomy, Valparaiso University, Valparaiso, IN, USA; wen.lu@valpo.edu, bruce.hrivnak@valpo.edu
Received 2006 June 28; accepted 2006 September 16

ABSTRACT

BD +42 2782 was recently discovered to be a variable star with a W UMa–type, eclipsing-binary light curve. We have obtained the first photoelectric light curves (R_C, I_C) and also the first radial velocity curves for this binary. These show the system to be a W UMa binary of the W type, with the less massive component eclipsed at primary minimum. The light and velocity curves have been analyzed in a consistent manner using the Wilson-Devinney synthetic light-curve code. The binary has an orbital inclination of 74°, a mass ratio of 0.4 … of 34%. Absolute paran … 7 $M_\odot$, $R_2 = 0.95\ R_\odot$, L … fer between the two con … ns to explain this are ex…

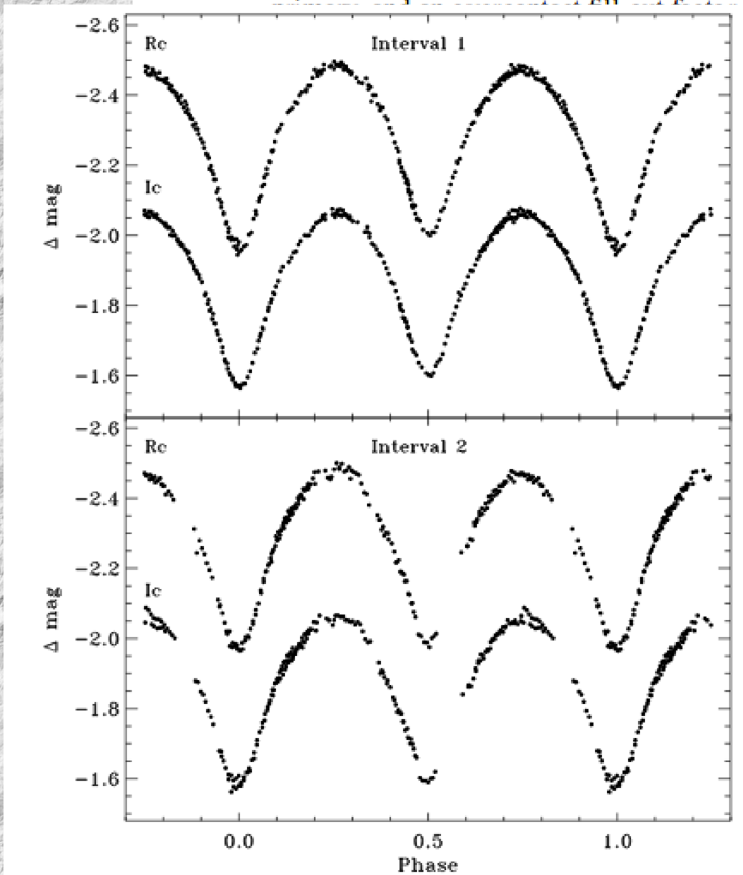

Fig. 1.—Differential light curves of BD +42 2782 from observing intervals 1 and 2 in 2004.

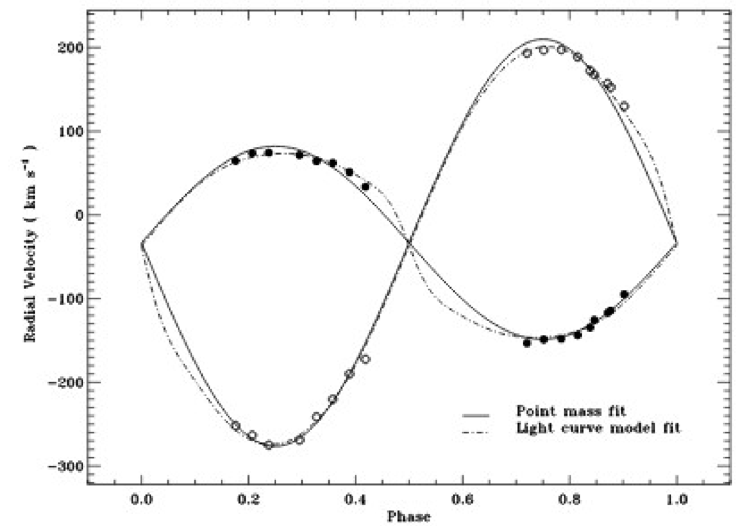

Fig. 2.—Radial velocity of BD +42 2782. Shown are the observations, along with the fits based a point-mass solution and the light-curve solution.

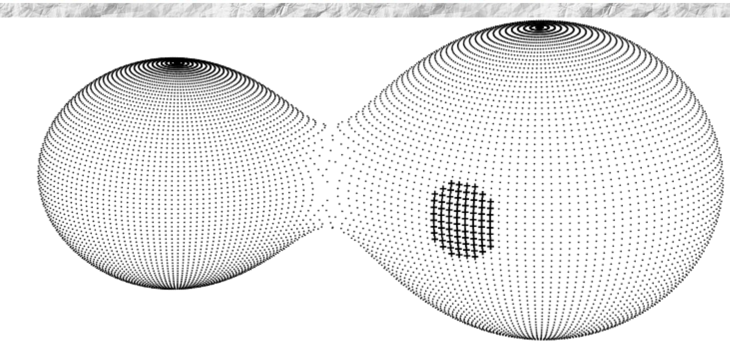

Fig. 4.—Model of the binary surface as seen at phase 0.75 *P*, showing the location of the cool spot.

Relación masa-luminosidad (secuencia principal)

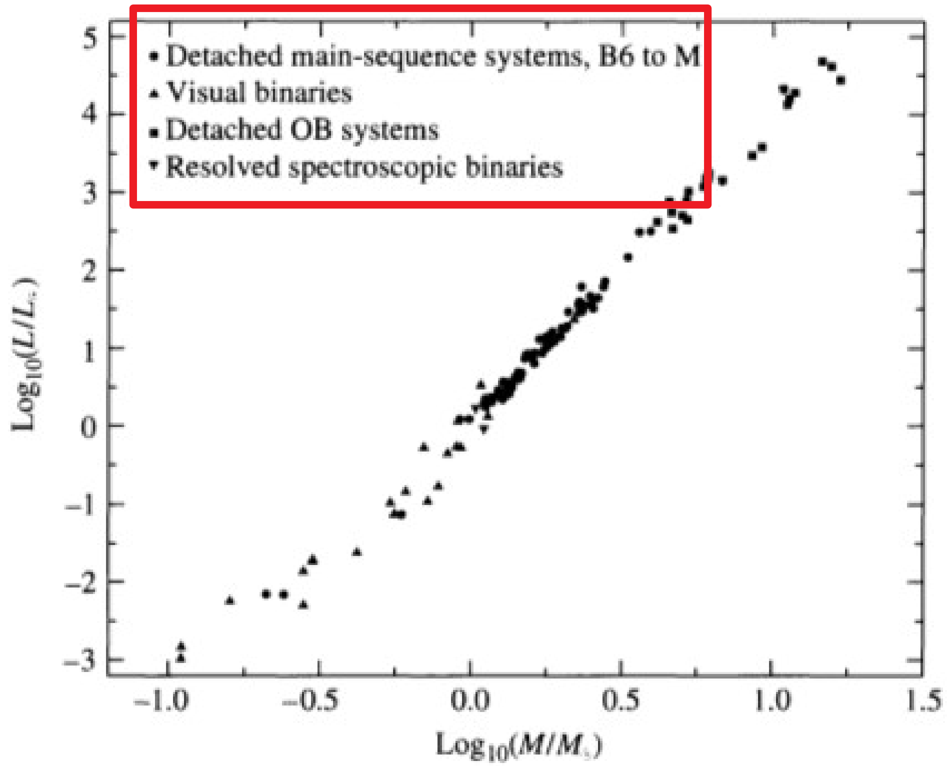

FIGURE 7.7 The mass–lu … *. Rev. Astron. Astrophys.*, *18*, 115, 1980.)

$$\frac{L}{L_\odot} \approx \left(\frac{M}{M_\odot}\right)^{3.5}$$

Relación masa-luminosidad (secuencia principal)

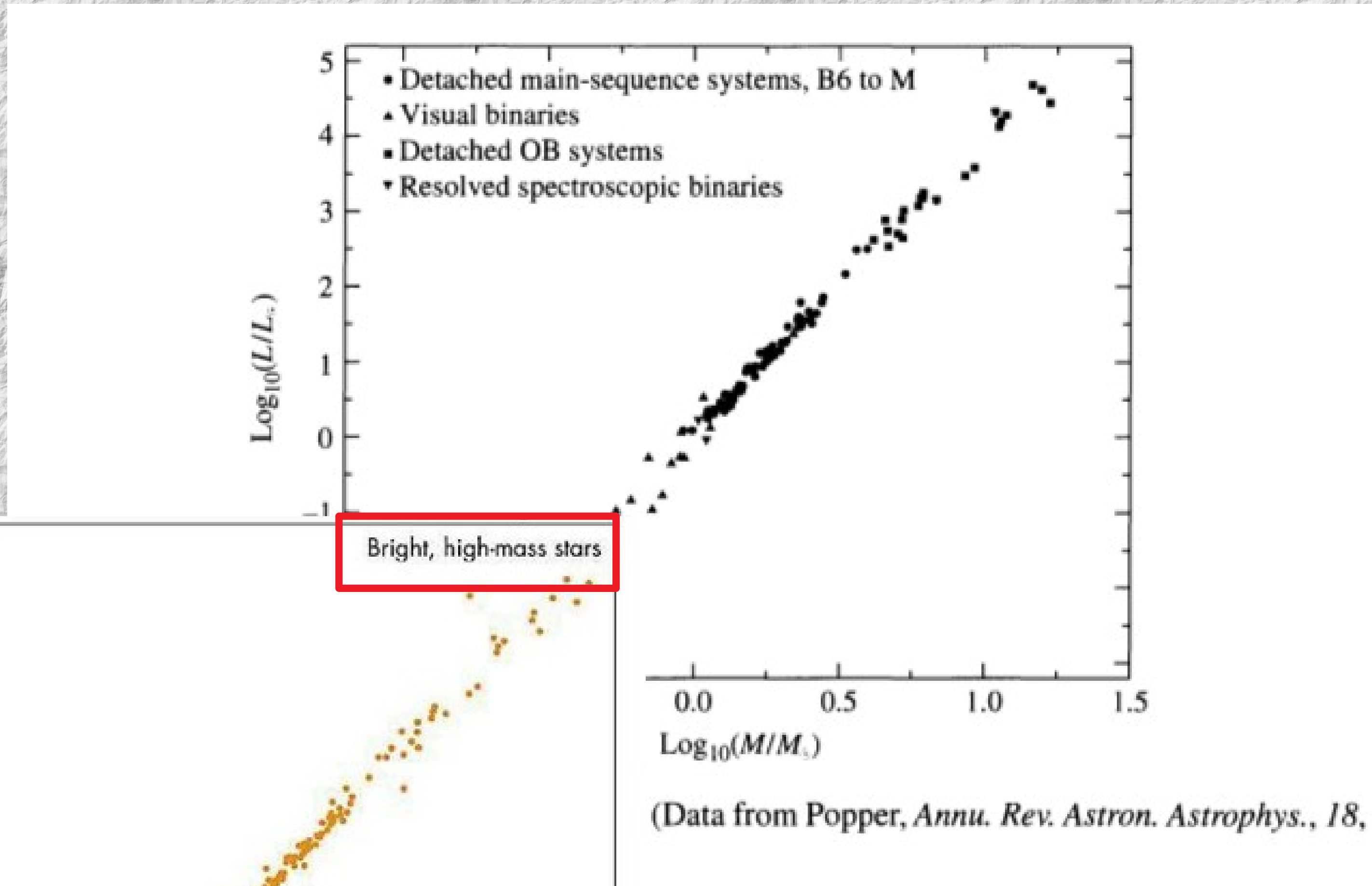

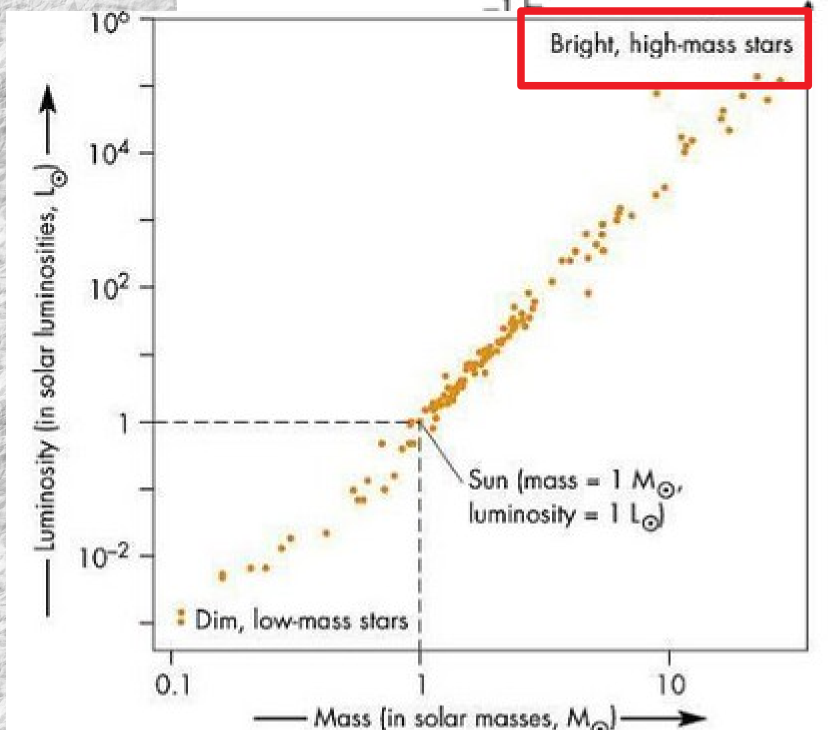

$$\frac{L}{L_{\Theta}} \approx \left(\frac{M}{M_{\Theta}}\right)^{3.5}$$